Aus der Klinik für Dermatologie, Venerologie und Allergologie
Prof. Dr. med. M. P. Schön
der Medizinischen Fakultät der Universität Göttingen

Shear Stress and NETosis

INAUGURAL-DISSERTATION

zur Erlangung des Doktorgrades
der Medizinischen Fakultät der
Georg-August-Universität zu Göttingen

vorgelegt von

Lukas Frederik Mrowietz

aus

Kiel

Göttingen 2023

Dekan: Prof. Dr. med. W. Brück

Betreuungsausschuss

Betreuer: Prof. Dr. med. M. P. Schön

Ko-Betreuerin: Prof. Dr. S. Köster

Prüfungskommission

Referent: Prof. Dr. med. M. P. Schön

Ko-Referent*in: ……

Datum der mündlichen Prüfung: ……

Hiermit erkläre ich, die Dissertation mit dem Titel "Shear Stress and NETosis" eigenständig angefertigt und keine anderen als die von mir angegebenen Quellen und Hilfsmittel verwendet zu haben.

Göttingen, den …… ……

(Unterschrift)

Table of content

List of figures

List of tables

List of abbreviations

CD	cluster of differentiation
cGMP	cyclic guanosine monophosphate
CitH3	citrullinated histone H3
CR3	complement receptor 3
DNA	deoxyribonucleic acid
ESL-1	E-selectin ligand-1
FCS	fetal calf serum
FPR	formyl peptide receptor
GP	glycoprotein
fMLP	N-formyl-methionyl-leucyl-phenylalanine
HBSS	Hank's Balanced Salt Solution
HEPES	4-(2-hydroxyethyl)-1-piperazineethanesulfonic acid
ICAM-1	intercellular adhesion molecule-1
ICAM-2	intercellular adhesion molecule-2
IL-1β	interleukin-1β
LCNM	live cell NETosis medium
LFA-1	lymphocyte function-associated antigen 1
LPS	lipopolysaccharides
Mac-1	macrophage-1 antigen
MAPK	mitogen-activated protein kinase
MPO	myeloperoxidase
NAPDH oxidase	nicotinamide adenine dinucleotide phosphate oxidase
NE	neutrophil elastase
NET	neutrophil extracellular trap
Orai1	calcium release-activated calcium channel protein 1 (encoded by ORAI1 gene)
P1-3	phase 1-3
Pa	pascal
PAF	platelet-activating factor
PBS	phosphate-buffered saline
PFA	paraformaldehyde
PKC	protein kinase C
PMN	polymorphonuclear leucocyte
PMA	phorbol 12-myristate 13-acetate
PSGL-1	P-selectin glycoprotein ligand-1
ROS	reactive oxygen species
SHR	spontaneous hypertensive rat
TNF-α	tumor necrosis factor-alpha
UV-A	ultraviolet A
VCAM-1	vascular cell adhesion molecule-1
VSMC	vascular smooth muscle cell

1 Introduction

1.1 The human immune system

The human immune system is a fine-tuned machinery with many components working together to ensure an effective protection against pathogens and danger signals in general. It is classically composed of two major parts: innate and adaptive immunity. Both are highly interconnected forming a specialized network to protect the body against various threats. The innate immune system consists of cellular and humoral components. On the cellular level, leukocytes like macrophages, neutrophil, eosinophil and basophil granulocytes and innate lymphoid cells neutralize and eliminate pathogens and thus function as a first-line immune defense while at the same time activating the adaptive immune system. These cells are supported by the complement system. The adaptive immune system also contains cellular and humoral components. Its cellular part mainly consists of lymphoid T- and B-cells which are responsible for a very effective, pathogen-specific immune response that is mediated via cellular killing mechanisms and antibody production (Murphy 2012).

1.2 Neutrophil granulocyte cell structure

Neutrophil granulocytes, commonly referred to as neutrophils, are a type of myeloid leukocytes. They measure 10 - 15 μm in diameter and show a characteristic polymorphic nucleus (Borregaard 2010). In the cytoplasm they hold four different kinds of granules: azurophilic, gelatinase, and specific granules, as well as secretory vesicles. The granules contain a variety of soluble and membrane-bound molecules that are essential for certain processes inside and outside of the cell (Cowland and Borregaard 2016). On their cell surface neutrophils express various molecules to communicate with other cells, to detect pathogens, and to ensure cell adhesion and migration (van Rees et al. 2016).

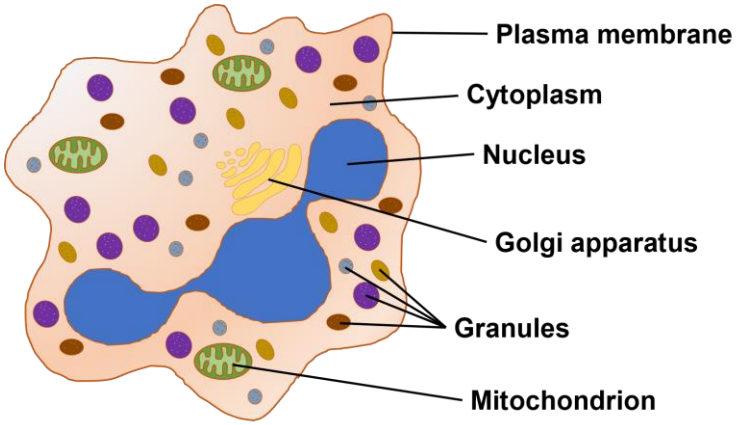

Fig. 1: Neutrophil granulocyte morphology. As their most prominent characteristic, neutrophils display a lobulated nucleus and neutrophil granules. Four different kinds of granules are known to be present in neutrophil cytoplasm: azurophilic granules, gelatinase granules, secretory granules, and secretory vesicles.

The nucleus of neutrophils is shaped in a polymorphic fashion. Each nucleus consists of three to four lobuli that are connected via a nucleoplasm bridge. Depending on the activation level of the neutrophil the lobulation can change (Skinner and Johnson 2017). The deoxyribonucleic acid (DNA) is stored inside the nucleus either as euchromatin or heterochromatin. Euchromatin consists of unbound DNA that is easily accessible for transcription and thus marks the active compartment in the nucleus. Heterochromatin refers to densely packed DNA that has bound to histones to maintain their supercondensed form. In the center of the nucleus lies a third layer, the inter-chromatin compartment, which does not contain any DNA (Hübner et al. 2015). The supercondensed DNA in the heterochromatin is organized in nucleosomes by the interaction between DNA and histones. Units of histone octamers are capable of binding 147 base pairs of DNA (Richmond and Davey 2003). Nucleosomes play an important role in the regulation of DNA. By phosphorylation, methylation, citrullination, ubiquitinylation, and acetylation, histones can be modified, which changes their binding properties. Transcription and DNA condensation can be regulated accordingly (Kouzarides 2007). The chromatin is surrounded by the nuclear envelope building a protective barrier. It comprises the inner nuclear membrane, the perinuclear space, and the outer nuclear membrane (Olins et al. 2008). Molecular exchange and transport occurs through nuclear pores (Beck and Hurt 2017).

The nucleus enables neutrophils to undergo complex processes like migration through tissues and extravasation through confined compartments between (or within) endothelial cells. Migratory processes have recently been found to be highly dependent on nuclear function. A complex sequence of cellular and nuclear rearrangements allows neutrophils to squeeze through compartments smaller than their own size and builds up intracellular forces that are necessary for progressive movement (Manley et al. 2018). Another process that is highly dependent on the nucleus is the creation of neutrophil extracellular traps (NETs),

commonly referred to as NETosis, a specialized mode of programmed cell death used in pathogen defense.

1.3 The role of neutrophils in immunity

As part of the innate immunity neutrophils are produced in the bone marrow and thereafter enter blood circulation. They can be part of a central pool, moving through the vessels alongside erythrocytes, platelets, and other components of the blood with the flow. Neutrophils can also attach to the blood vessel walls, entering a marginal pool. This process is regulated by the endothelium in post-capillary venules.

To fight pathogens, neutrophils are recruited from the blood circulation to the site of infection (de Oliveira et al. 2016). This process is regulated in a complex way. Under physiological conditions, endothelial cells express the adhesion molecules E- and P-selectin on their luminal surface, also referred to as CD62E and CD62P by the Cluster of Differentiation (CD) nomenclature. Neutrophils can bind to these proteins via P-selectin glycoprotein ligand-1 (PSGL1/CD162), resulting in a rolling movement, typically but not necessarily in the direction of flow (Zarbock et al. 2011). After pathogen encounter or danger signal activation from the tissue of the vascular microenvironment, endothelial cells express a second class of adhesion molecules, such as intercellular adhesion molecule 1 (ICAM-1/CD54) and 2 (ICAM-2/CD102) and vascular cell adhesion molecule 1 (VCAM-1/CD106). When rolling neutrophils get stimulated, they express and bind through integrins, such as β1-integrins (ITGB1/CD29) and β2-integrins (ITGB2/CD18) (Phillipson et al. 2006). This binding leads to an arrest of the rolling movement and a flattening of the neutrophil, ultimately resulting in strong attachment to the endothelial cells and para- or transcellular migration through the endothelium (Garrido-Urbani et al. 2008). After entering the extravascular space, neutrophils follow a chemotactic gradient to actively migrate to the site of infection and/or inflammation (Kolaczkowska and Kubes 2013).

Once in contact with pathogens, neutrophils provide different defense mechanisms, such as phagocytosis, degranulation, release of reactive oxygen species (ROS), and NETosis. Selection of these mechanisms depends, among other factors, on the pathogen encountered. Pathogen associated molecules like lipopolysaccharides (LPS) and microbe size are factors that trigger specific defense strategies of neutrophils (Papayannopoulos 2018). One group found microbe size to be the defining factor on whether neutrophils engage in phagocytosis or NETosis after contact (Branzk et al. 2014). In the following, these neutrophil defense mechanisms are explained in greater detail.

1.3.1 **Phagocytosis**

Phagocytosis describes the internalization of pathogens in phagosomes. If a pathogen is opsonized by antibodies or complement, neutrophils can initiate phagocytosis via extended

pseudopods (Abram and Lowell 2007). Once pathogenic material is phagocytosed, azurophilic granules can fuse with phagosomes to ensure a fast and efficient degradation. Another way to degrade phagocytosed material is by the production and release of ROS by Nicotinamide adenine dinucleotide phosphate oxidase (NADPH oxidase) activity (Tapper 1996).

1.3.2 **Degranulation**

Neutrophils hold four different types of granules in their cytoplasm: azurophilic, gelatinase, and specific granules, as well as secretory vesicles. All granules contain potentially effective molecules to degrade pathogens, however, the azurophilic granules show much higher concentration of proteolytic enzymes and are primarily activated in pathogen-associated reactions. The most important substances involved in this process are myeloperoxidase, neutrophil elastase, neutrophil serine protease 4, proteinase 3, cathepsin G, lysosomal proteins, bactericidal/permeability-increasing protein, and defensins (Egesten et al. 1994). Azurophilic granules can fuse with phagosomes. In addition, neutrophils can engage in degranulation in which the granules fuse with the cell membrane to release the granules' content into the extracellular space (Bedouhène et al. 2020). Besides the direct effect on pathogens, degranulation plays a very important role in the coordination of immune reactions but also in unspecific tissue damage. By releasing not only pathogen effectors but also chemoattractants and proinflammatory molecules, neutrophils can trigger strong immunological reactions (Kolaczkowska and Kubes 2013).

1.3.3 **ROS**

ROS are commonly referred to as highly reactive molecules containing oxygen which has a high electron acceptability. Among them, superoxide anions (O_2^-), hydrogen peroxide (H_2O_2), hypochlorous acid (HClO), and hydroxyl radicals (OH) play a role in neutrophil-related ROS production (Hampton et al. 1998). Upon assembly of NADPH oxidase in the phagosomal, granular, or plasma membrane and during phagocytosis activation or stimulation with compounds like phorbol 12-myristate 13-acetate (PMA) and N-formyl-methionyl-leucyl-phenylalanine (fMLP), the enzyme starts to produce superoxide anions. Subsequently, other ROS are formed most notably hydrogen peroxide which is a substrate for myeloperoxidase (MPO) (Aratani 2018). ROS generation can be utilized as a direct effector against pathogens. It is also part of many intracellular pathways including NETosis (Vorobjeva and Chernyak 2020).

1.3.4 **NETosis**

First described in 1996 as "changes different from typical apoptosis or necrosis" (Takei et al. 1996), NETs did not become a scientific focus until in 2004 Brinkmann et al. identified this process as a separate defense mechanism of neutrophils, distinct from degranulation and

phagocytosis. They observed neutrophils releasing decondensed chromatin in web-like structures decorated with antimicrobial proteins and granular molecules, such as elastase, in response to bacteria (gram positive/negative), LPS, and PMA. They minted the term "neutrophil extracellular traps (NETs)" (Brinkmann et al. 2004). Upon stimulation with compounds such as PMA, LPS, calcium-ionophore, urate crystals, or candida albicans hyphae, neutrophils engage in NETosis (Papayannopoulos 2018). Depending on the stimulus, different pathways are activated, ultimately resulting in the degradation of the cytoskeleton and the modification of histones weakening their binding properties to the DNA. Once the DNA loses its strong bond to histones, it starts to expand inside the nucleus. With the onset of DNA swelling, the nuclear envelope cannot withstand the pressure and eventually ruptures, releasing DNA into the cytoplasm. Chromatin expansion continues until finally the cell membrane ruptures and the expanded DNA meshwork, covered with nuclear and cytoplasmic proteins, is expelled as a NET into the extracellular space (Neubert et al. 2018; Vorobjeva and Chernyak 2020). In a recent publication, our group showed that the whole process of NETosis can be divided into three distinct phases, as shown in Fig. 2. The first phase P1 starts with the administration of a potent NETosis-stimulus and ends at timepoint t1 at which chromatin swelling starts. Starting from t1, phase P2 describes the chromatin expansion inside the cytoplasm with a maximal expansion area at timepoint t2, followed by a slight decrease and rounding of the cell body. Phase P2 ends at timepoint t3 with the rupture of the cell membrane and expulsion of the NET, marking the start of phase P3 (Neubert et al. 2018). Our group found that P1 is an active enzymatic, energy-dependent process that is influenced by many factors intracellularly, while P2 and P3 are passive irreversible processes that are driven by properties of the DNA-material. Once the chromatin is no longer tightly bound to histones, entropic forces drive DNA-swelling (Neubert et al. 2018).

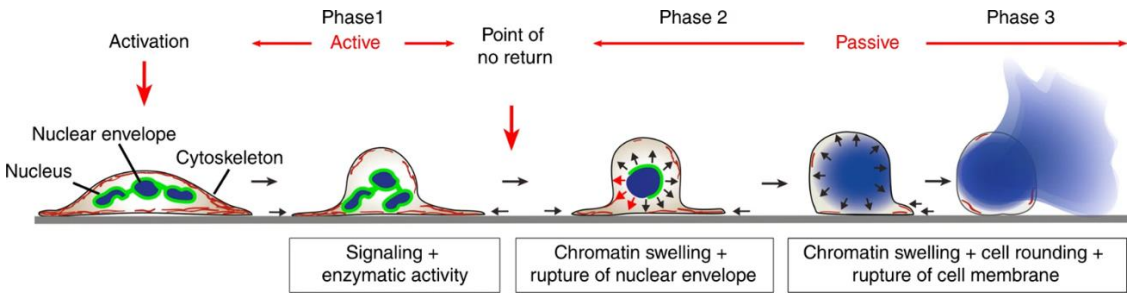

Fig. 2: The process of NETosis and its different phases. (Neubert et al. 2018), (license: CC BY 4.0)

In order to detect NETs *in vitro* and *in vivo* in contrast to free DNA, different biomarkers have been discovered. Among them citrullinated histone H3 (CitH3), which is a byproduct of NETosis and bound to the released DNA, has proven to be one of the most reliable and specific biomarkers, used by a great number of studies (Rochael et al. 2015; Bryk et al. 2019; Neubert et al. 2019; Pertiwi et al. 2019; Kuczia et al. 2020).

1.3.5 **PMA induced NETosis**

NETosis can be triggered by a wide range of stimuli. Depending on the stimulus, the pathways ultimately leading to degradation of the cytoskeleton and modification of histones show some differences to one another. However, most pathways eventually activate NADPH-oxidase which produces ROS and in return activates MPO. MPO activates neutrophil elastase (NE) and contributes to its translocation from azurophilic granules into the nucleus, where NE proteolytically modifies histones (Vorobjeva and Chernyak 2020). NE that is released into the cytosol cleaves cytosolic F-actin and thereby degrades the cytoskeleton (Metzler et al. 2014). A commonly used stimulus for NETosis is PMA. PMA activates protein kinase C (PKC) which in turn activates NADPH oxidase, inducing production of ROS. ROS then activate mitogen-activated protein kinase p38 (MAPK p38) as it has been shown in mouse neutrophils (Saito et al. 2005). These complex pathways remain poorly understood and more evidence is needed to support these findings.

1.4 NETs in autoimmunity and disease

Apart from the beneficial effects of NETs in host defense they are associated with a variety of non-infectious diseases such as cystic fibrosis (Papayannopoulos et al. 2011), deep vein thrombosis (Brill et al. 2012; Diaz et al. 2013), atherosclerosis (Warnatsch et al. 2015), ischemia reperfusion injury (Raup-Konsavage et al. 2018), Alzheimer disease (Zenaro et al. 2015), systemic lupus erythematosus (Leffler et al. 2013), rheumatoid arthritis (Wang et al. 2018), psoriasis (Hu et al. 2016; Schön and Erpenbeck 2018), cancer (Erpenbeck and Schön 2017; Kim et al. 2018), and COVID-19 (Barnes et al. 2020). The role of NETs in the pathogenesis of these diseases remains poorly understood. One study found that neutrophils exposed to cholesterol crystals that can be found in atherosclerotic plaques are stimulated to undergo NETosis. These NETs promote other immune cells like macrophages to produce pro-inflammatory cytokines (Warnatsch et al. 2015).

1.5 NETosis and shear stress

Neutrophils in the marginal pool of the vascular system are constantly exposed to shear stress created by pressure of the blood flow on the neutrophil's surface. Shear stress is pressure applied to an area by a tangential force, known as shear force. In fluidic setups, shear force is generated at cross-sectional contact between moving fluid and its surrounding as exemplified in Fig. 3.

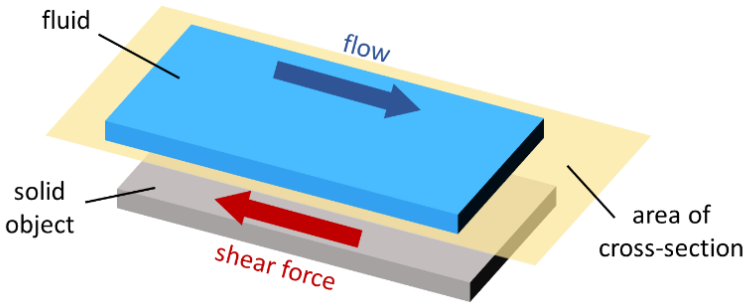

Fig. 3: Schematic shear force model. The model displays how moving fluid creates shear force on an adjacent solid object.

Whenever an adherent cell is exposed to moving fluids, shear stress occurs depending on the intensity of the shear rate and the contact area of the cell. If not used to describe adherent cells or other objects, the term 'shear stress' usually refers to wall shear stress of blood vessels. Shear stress is measured in pascal (Pa). The following formulas describe mathematical dependencies of shear stress, shear rate, and shear force:

$$\tau = \frac{F_S}{A} = \eta * \gamma \qquad \gamma = \frac{\Delta v}{\Delta h} \qquad F_s = \tau * A$$

$\tau = shear\ stress$ $\eta = viscosity$ $v = velocity$ $F_s = shear\ force$
$\gamma = shear\ rate$ $A = area$ $h = height$

Eq. 1: Formulas describing the mathematical dependencies of shear stress.

These formulas apply to conditions of laminar flow with Newtonian fluid with very small Δh. In order to manipulate shear stress in an experimental setup, many variables can be modified such as increasing viscosity of the fluid or perfusion rate, resulting in an increase of shear stress.

The physiological range of shear stress occurring in the vascular system in humans varies strongly from < 0.1 to > 15 Pa (Malek et al. 1999; Cheng et al. 2002). These differences are due to the anatomical architecture of the circulatory system. Shear stress is normally higher in arteries in comparison to veins. Malek et al. measured shear stress in different blood vessels, ranging from 1 to 7 Pa in the arterial vascular network and from 0.1 to 0.6 Pa in the venous system (Malek et al. 1999). An important factor influencing shear stress is the vessel's diameter. With increasing diameter shear stress decreases. As an example, shear stress in the human abdominal aorta ranges from 0.23 - 0.34 Pa in comparison to shear stress at arterial level with smaller diameter (> 1.5 Pa) (Malek et al. 1999; Cheng et al. 2002). To understand the quantity of shear stress exposure to neutrophils, capillaries and post capillary venules play an important role. Migration into surrounding tissue happens in the latter, preceded by

neutrophils entering the marginal pool and thus becoming exposed to shear stress. While the mean wall shear stress value for such microvessels was shown to be 1.54 Pa in one study examining human conjunctival microvessels, the variation strongly depended on the vessels' diameter in a hyperbolic fashion with values ranging from 9.55 Pa in the smallest capillaries to 0.28 Pa in the higher diameter post capillary venules (Koutsiaris et al. 2007).

Another factor defining shear stress intensity is the flow rate: the higher the flow rate, the higher the shear stress. This was exemplified by Cheng et al. measuring shear stress in the abdominal aorta of healthy human volunteers that either engaged in physical exercise (thereby increasing heart rate and blood flow rate) or rested. Results showed an increased shear stress during exercise (men, 0.51 +/- 0.08 Pa; women, 0.54 +/- 0.21 Pa) in comparison to resting (men, 0.12 +/- 0.05 Pa; women, 0.14 +/- 0.07 Pa) (Cheng et al. 2003).

The above-mentioned values have been measured using different methods like shear stress quantification from axial red blood cell velocity in vessels of known geometry and flow profile using a slit lamp based imaging system (Koutsiaris et al. 2007), and computational analysis and calculation of magnetic resonance imaging data (Cheng et al. 2002).

Recently, a study has shown that high shear stress applied to neutrophils can induce NETosis (Yu et al. 2018). In their experiments, microchannels perfused with human whole blood to form occlusive thrombi were used. After perfusion with whole blood through these thrombi at venous and arterial pressure gradients, neutrophils and DNA were fixed and stained. In areas where neutrophils were exposed to shear stresses exceeding 15 Pa, described as the "known lytic value" (Dewitz et al. 1977), DNA was expelled and NETosis was verified by confirming NETs to be immunopositive for citrullinated histone H3. Albeit CitH3 being a widely used diagnostic tool to discriminate between free DNA and NETs, not all NETs in these experiments were CitH3 positive. While this observation showed that shear stress might be a potent inducer for NETosis, the process itself has not yet been investigated under flow conditions. With the aforementioned established technology to discriminate between different NETosis phases, a new method became available to investigate this process.

1.6 Aims of the work

The present study aimed to investigate how shear stress influences NETosis as such and the different phases of NETosis in human neutrophils. A new experimental setup inspired by recent discoveries on the differentiation of NETosis phases was established. Human neutrophils in *in vitro* flow chambers were either pre-exposed or exposed to continuous shear stress, and subsequently stimulated to undergo NETosis, followed by three to four hours of live cell imaging. The data was used to extrapolate the findings for physiological and pathophysiological concepts.

2 Materials and methods

To investigate the different effects of shear stress on the process of NETosis in human neutrophils, different experimental setups were established.

2.1 Isolation of human PMN

Human neutrophils were isolated from three anonymous healthy donors (2 male and 1 female, aged between 20-29 years, all non-smokers). This study was carried out in accordance with the recommendations and with the approval of the Medical Ethics Committee of the University Medical Center Göttingen (UMG), protocol number 29/1/17 with written informed consent from all subjects and in accordance with the Declaration of Helsinki. The isolation procedure was conducted after previously published standard protocols (Neubert et al. 2018).

In short, fresh peripheral venous blood was collected, using S-Monovettes KE 7.5 ml (Sarstedt, Nümbrecht, Germany). On top of Histopaque 1119 (Sigma-Aldrich, Taufkirchen, Germany), blood was layered in a 1:1 ratio in 15 ml Falcon tubes (Corning, Kaiserslautern, Germany). The tubes were centrifuged at 1100 x g for 21 min. The third layer (transparent) and the fourth layer (pink) contained the white blood cells. Both layers were removed and mixed with 1 x Hanks' Balanced Salt Solution (HBSS) -/- (Thermo Fisher Scientific, Osterode am Harz, Germany). Cells were centrifuged at 400 x g for 10 min to form a pellet. The supernatant was removed and the pellet was resuspended in HBSS -/-. The cells were gently layered on top of a phosphate buffered Percoll (GE Healthcare, Solingen, Germany) gradient with concentrations of 85, 80, 75, 70, and 65 percent. The tube was centrifuged at 1100 x g for 22 min. Neutrophils accumulated predominantly in the 75% layer. Therefore, half of the 70%, all of the 75%, and half of the 80% layer were collected and mixed with 1 x HBSS -/-. To form a pellet the cells were centrifuged at 400 x g for 10 min at room temperature. The supernatant was discarded and the cells were resuspended in 500 µl HBSS -/-. An aliquot was used to count the cells using a Neubauer chamber. The required number of cells was suspended in experimental buffer, according to the setup. Purity of the cell-suspension was confirmed by a Shandon Cytospin 2 centrifuge sample (Epredia, Kalamazoo, USA) followed by Diff Quick staining (Medion Diagnostics, München, Germany). Cell purity of isolated neutrophils used in the experiments was >95% (Neubert et al. 2018).

2.2 Medium for live cell NETosis assays

In live cell experiments with neutrophils, the composition of the medium is essential for the viability of the cells. However, not all ready-to-use whole-media that are commonly used with neutrophils proved to be suitable for our experiments. Four aspects were taken into

account to find a proper medium: the light effect, neutrophil adhesion, spontaneous NETosis, and neutrophil viability.

The light effect describes an Ultraviolet A (UV-A) or blue-light triggered generation of ROS via the excitation of riboflavin in cell media. ROS in turn trigger NETosis. This effect is even stronger in presence of 4-(2-hydroxyethyl)-1-piperazineethanesulfonic acid (HEPES), a commonly used buffer (Neubert et al. 2019). Since the DNA-stain HOECHST 33342 is excited by blue-light, a medium devoid of Riboflavin and HEPES needed to be established to prevent light induced NETosis during live cell imaging. Addressing cell adhesion, one of the most important aspects is the pH. In an acidic microenviroment, physiologically present in inflamed or ischemic tissues, neutrophils showed stronger CD18-dependent adhesion in comparison to a basic microenviroment (Serrano et al. 1996). In the present study, a pH of 7.2 proved to be sufficient. Since spontaneous NETosis rates reported to be lower in media with serum components than without, heat inactivated fetal calf serum (FCS) was used to prevent this effect (Neubert et al. 2019). Considering these requirements, a minimalistic medium with HBSS +/+ to provide all essential ions and nutrition and an inherent salt-based buffer, FCS to prevent spontaneous NETosis, and a pH of 7.2 titrated with hydrochloric acid (HCl) to ensure optimal cell adhesion, was composed. This live cell NETosis medium (LCNM) proved to be sufficient in all four aspects. Its composition is described in detail in the following.

50 ml samples were prepared by mixing 250 µl 100% FCS (heat-inactivated at 56°C) (Sigma-Aldrich, Taufkirchen, Germany) and 49.75 ml 1x HBSS +/+ (with Ca ++ and Mg ++, without phenol red, for details see Tab. 1.) (Lonza, Köln, Germany). The pH was titrated to 7.2 by adding 1 M HCl (Carl Roth, Karlsruhe, Germany) measured with a pH-meter (FiveEasy FE20, Mettler-Toledo, Gießen, Germany). The medium was sterile-filtrated through a 0.2 µm syringe-filter (Filtropur S plus 0.2, Sarstedt, Nümbrecht, Germany). All samples were stored either at 4°C when used within three days or otherwise stored at -20°C.

Tab. 1: Formulation of 1x HBSS.

Description	Concentration (g/L)	Molarity (mM)
Calcium Chloride Dihydrate	0.186	1.265
Dextrose	1	5.551
Magnesium Sulfate Heptahydrate	0.2	0.811
Potassium Chloride	0.4	5.366
Potassium Phosphate Monobasic Anhydrous	0.06	0.441
Sodium Bicarbonate	0.350	4.166
Sodium Chloride	8	136.893
Sodium Phosphate Dibasic-7-Hydrate	0.09	0.336

Formulation of 1x HBSS +/+ (with Ca ++ and Mg ++, without phenol red) (Lonza, Köln, Germany).

2.3 Setup 1: Analysis of human neutrophils during NETosis under low continuous shear stress

In the first set of experiments, human neutrophils were isolated from healthy donors, seeded into a flow-chamber, stained with a live cell DNA dye, and washed. The flow chamber was connected to a circular pump that ensured a continuous flow with low shear stress. While under flow, the cells were stimulated with PMA, a well-established NETosis-stimulus (Papayannopoulos 2018). The cells were imaged live under an inverted fluorescence microscope (Axiovert 200, Zeiss, Oberkochen, Germany) for three hours. The resulting data was analyzed by the naked eye and by a program specifically designed for this purpose described in detail in chapter 2.6.

2.3.1 Cell preparation

250 000 purified human neutrophils were resuspended in 500 µl LCNM. 200 µl of this cell suspension were filled into a flow chamber (µ-Slide I Luer; Surface Modification: ibiTreat: #1.5 polymer coverslip, tissue culture treated, sterilized; Channel Height: 0.8 mm; ibidi GmbH, Gräfelfing, Germany). The reservoir used as inlet was marked. Every application of fluid from this point used this reservoir as inlet. The flow chamber was incubated in a cell culture incubator for 30 minutes at 37°C and 5% CO_2 to let the cells adhere. Adhesion was controlled under an inverted microscope (Axiovert 40c, Zeiss, Oberkochen, Germany). After adhesion, the cells were stained with HOECHST 33342 (Thermo Fisher Scientific, Osterode am Harz, Germany), a live cell DNA dye in a dilution of 1:2500 in LCNM. To apply the solution, two micropipettes (Brand, Wertheim, Germany) were used. With one pipette, 200

µl of the dye solution were filled into one side of the flow chamber while simultaneously removing 200 µl from the other side with the second pipette. This handling was used in all flow chamber experiments for exchanging fluid. The flow chamber was kept in the incubator for 15 minutes at 37°C and 5% CO_2 for the dyeing procedure. Afterwards, the flow chamber was washed with 200 µl LCNM, using the same procedure for exchanging fluid as described above. Both reservoirs were filled with 50 µl LCNM each to prevent the chamber from drying out. The chamber was stored in the incubator for 20 minutes at 37°C and 5% CO_2. To ensure tube connection without air bubbles entering the system, the reservoirs were filled up completely with LCNM after incubation prior to connecting the tubes.

2.3.2 **Circular pump setup**

To mimic constant shear stress as in venous conditions in humans, a circular pump system was used (ibidi Pump System; Ibidi GmbH). To ensure a gradual upshift of shear stress on the cells, the pump was programmed to increase the flow stepwise resulting in an upshift of shear stress from 0.1 Pa to 0.5 Pa in 10 seconds. Perfusion then remained constant to ensure a shear stress of 0.5 Pa.

The tube system was either rinsed with 70% ethanol and distilled water or autoclaved prior to use. A perfusion set (Perfusion Set – yellow and green; length: 50 cm; Inner Diameter: 1.6 mm; ibidi GmbH) was used. The perfusion set was installed into the pump according to the manual.

A heating chamber (ibidi Heating System, Universal Fit, for 1 Chamber; Product Variation: With heated lid; ibidi GmbH) was used.

PMA was added up to a concentration of 100 nM into 20 ml LCNM. This buffer was heated to 37°C in a water-bath. The buffer was transferred into the perfusion set 25 minutes prior to perfusion. It was added until both syringes were filled to the 6 ml mark. In order to remove air from the system the pump was set to 0.8-chambers, shear stress: 8 dyn infinite, and switching time: 8 s. It was turned on until all air was removed. The program was then set to 0.8-chambers, shear stress: shift up 1 – 5 dyn (P1: 1 dyn for 5s, P2: 3 dyn for 5s, P3: 5 dyn infinite) and switching time: 15 s in P3.

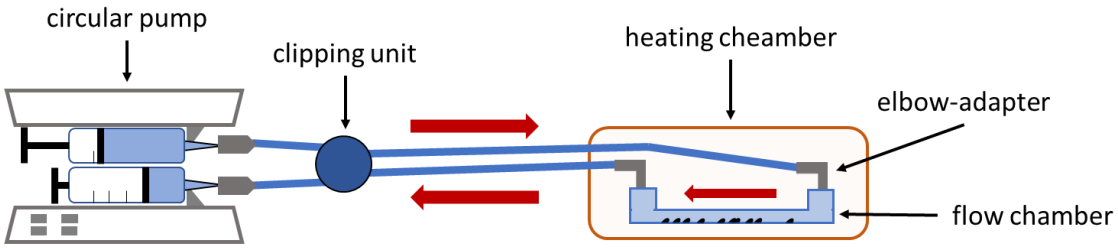

Fig. 4: Schematic overview of the circular pump setup. Red arrows mark the direction of flow.

2.3.3 Stimulation, perfusion & imaging

Ten minutes prior to perfusion the flow chamber was installed into the heating chamber. The perfusion set was connected to the heating chamber. With careful handling to avoid air entering the system the inlet tube was connected first. Thereafter, the outlet tube was connected. While connecting, both tubes were clamped distal of the elbow connectors. Under the microscope an area in the center of the flow chamber was selected. While searching for an area with even neutrophil distribution, light exposure was minimized as much as possible to prevent light induced NETosis. Stimulation and imaging started simultaneously at t = 0 min. After 3-4 hours of imaging the flow chamber was disconnected from the tubing and filled with 200 µl 4% Paraformaldehyde solution (PFA, Roth). The flow chamber was stored at 4°C in the dark.

2.3.4 Microscope setup

The aforementioned inverted microscope was used with 20 x magnification (EC Plan-Neofluar Ph1/440331-9901-000, Zeiss), fluorescent channel (Filter set 02 shift free/488002-9901-000, Zeiss) for 4',6-diamidino-2-phenylindole (DAPI) which, like HOECHST 33342, has an emission maximum at 461 nm. A camera (CoolSNAP ES, Photometrics, Surrey, Canada), a fluorescent lamp (HBO 100, Vincent Associates, Rochester, USA) and an automatic shutter (UNIBLITZ Model VCM-D1 Shutter driver, Visitron Systems, Puchheim, Germany) were used. The software (Metamorph 6.3r2, Molecular Devices, Zeiss) was fed with the following parameters: autoshutter: on, binning: 1, exposure: 60, and multi acquisition 1 image/min for 241 images.

2.3.5 Alternative conditions

Another condition was investigated with an application of flow resulting in a shear stress of 0.1 Pa. All steps and time points were performed and met exactly like in the setup with 0.5 Pa. The program for the circular pump was set accordingly: 0.8-chambers, shear stress: P1: 1 dyn infinite with switching time 15 s.

2.4 Setup 2: Analysis of human neutrophils during NETosis after pre-treatment with high shear stress

In the second set of experiments, human neutrophils were isolated from healthy donors, seeded into a flow-chamber, stained with a live cell DNA dye, washed, and connected to an unidirectional syringe-pump that ensured a high shear stress for five minutes to pre-treat the cells. After application of shear stress, the cells were stimulated with PMA. The cells were imaged live under an inverted fluorescence microscope for three hours. The resulting data was analyzed as in the first setup.

2.4.1 Cell preparation

One million purified human neutrophils were resuspended in 500 µl LCNM. 55 µl of this cell suspension were filled into a flow chamber (µ-Slide I Luer; Surface Modification: ibiTreat: #1.5 polymer coverslip, tissue culture treated, sterilized; Channel Height: 0.2 mm; ibidi GmbH). The reservoir used as inlet was marked. Every application of fluid from this point used this reservoir as inlet. The flow chamber was incubated in a cell culture incubator for 30 minutes at 37°C and 5% CO_2 to let the neutrophils adhere. Adhesion was controlled under an inverted microscope. After adhesion, the neutrophils were stained with HOECHST 33342, a live cell DNA dye at a dilution of 1:2500 in LCNM. To apply the solution, two 100 µl micropipettes (Brand) were used. With one pipette 60 µl of the dye solution were filled into one side of the flow chamber while simultaneously sucking out 60 µl from the other side with the second pipette. This procedure was used in all flow chamber experiments for exchanging fluid. The flow chamber was kept in the incubator for 15 minutes at 37°C and 5% CO_2 for the staining procedure. Thereafter, the flow chamber was washed with 60 µl LCNM using the same procedure for exchanging fluid as described above. Both reservoirs were filled with 50 µl LCNM each to prevent the chamber from drying out. The chamber was stored in the incubator for 25 minutes at 37°C and 5% CO_2.

2.4.2 Syringe pump setup

To mimic shear stress as in arterial conditions in humans, a syringe pump was used (AL-4000; Aladdin Programmable Double Syringe Pump; World Precision Instruments Germany GmbH, Friedberg, Germany). To ensure a gradual upshift of shear stress on the cells, the pump was programmed to increase the flow stepwise resulting in an upshift of shear stress from 0.1 Pa to 6.5 Pa in 17 seconds. Subsequently, perfusion was kept constant to ensure a shear stress of 6.5 Pa for 5 minutes. Afterwards perfusion was stopped.

Tab. 2: Syringe pump program.

Program	effective shear stress in Pa	mode	parameter r in ml/min	effective perfusion rate in ml/min	volume admitted in ml
P01	0.1	rate	0.1	0.1	0.003
P02	~ 0.3	incr	+ 0.3	0.4	0.01
P03	~ 0.5	incr	+ 0.3	0.7	0.02
P04	~ 1	incr	+ 0.8	1.5	0.05
P05	~ 2	incr	+ 1.5	3	0.1
P06	~ 3	incr	+ 1	4	0.13
P07	~ 4.3	incr	+ 2	6	0.2
P08	~ 5	incr	+ 1	7	0.23
P09	~ 5.8	incr	+ 1	8	0.26
P10	6.5	incr	+ 1.05	9.05	45.25
P11	/	stop	/	/	/

Program and parameters of the syringe pump for two 50 ml syringes (B. Braun, Melsungen, Germany) with an inner diameter of 30.5 mm.

The tube system was either rinsed with 70% ethanol and distilled water or autoclaved prior to use. The tubing (Silicone Tubing; Inner Diameter; 1.6 mm; ibidi GmbH) was cut into two short (5 cm) and two longer (30 cm) pieces. The two short pieces were attached to one syringe adapter (Luer Lock Connector Female; ibidi GmbH) each and connected via a Y-connector (Hose connectors ROTILABO® Mini Y-shape, Suitable for: Hose inner Ø 1.6 mm; Carl Roth) to one of the long pieces. The flow chamber was connected to both long pieces via elbow connectors (Elbow Luer Connector Male; ibidi GmbH). A heating chamber (ibidi Heating System, Universal Fit, for 1 Chamber; Product Variation: with heated lid; ibidi GmbH) was used. Two 50 ml syringes (Original Perfusor® Syringe 50 ml; Luer Lock; B. Braun) filled with 50 ml LCNM and heated to 37°C in a water bath were installed into the pump 15 minutes prior to perfusion. The tubing was connected to the syringes and by pre-pumping the inlet tubing was filled with medium to remove air bubbles.

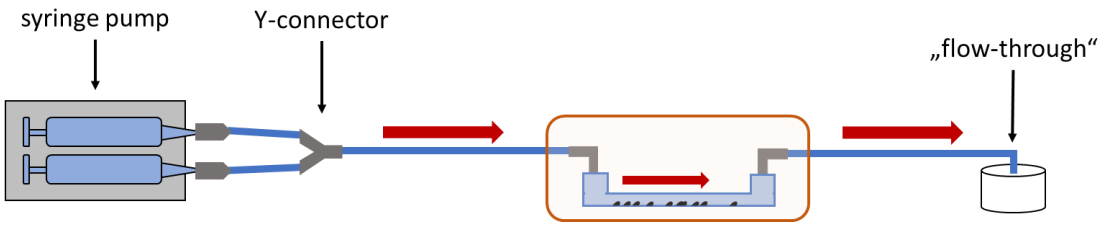

Fig. 5: Schematic overview of the syringe-pump-setup. Red arrows mark the direction of flow.

2.4.3 Perfusion

Five minutes before the perfusion started, the flow chamber was installed into the heating chamber. At first, the inlet tubing was connected to the flow chamber with careful handling to prevent air bubbles entering the system. Then the outlet tubing was connected. Under the microscope an area near the outlet on the flow chamber was selected. While searching for an area with even neutrophil distribution, light exposure was minimized as much as possible to prevent light induced NETosis. The microscope was set as described below. Imaging and perfusion started at the same time. After perfusion stopped, the outlet tubing and then the inlet tubing were gently disconnected from the flow chamber and it was stored in the incubator at 37°C, 5% CO_2.

2.4.4 Stimulation and imaging

Seven and a half minutes after the perfusion was stopped, neutrophils were stimulated with PMA. For this step, the residual medium was emptied from the outlet reservoirs of the flow chamber with a 100 µl micropipette. Then 100 µl of 100 nM PMA solution in LCNM were added into the flow chamber. This step was repeated to ensure a concentration of 100 nM PMA without dilution errors from residual medium. The flow chamber was reinstalled into the heating chamber. Under the microscope an area in the center of the flow chamber was selected. While searching for an area with even neutrophil distribution, light exposure was limited as much as possible to prevent light induced NETosis. 6 minutes after stimulation, imaging started. After 3 hours of imaging, the flow chamber was disconnected from the tubing and filled with 200 µl 4% PFA-solution (Roth). The flow chamber was stored at 4°C in the dark.

2.4.5 Microscope setup

The aforementioned microscope setup was used. The software was fed with the following parameters: autoshutter: on, binning: 1, exposure: 60 (50 during perfusion), and multi acquisition 181 images with 1 image / min.

2.5 Control setup

2.5.1 Control setup without application of flow

In this control setup, the flow chamber was transferred into the heating chamber but stayed unconnected from any tubing. Except for that, all steps and timepoints were performed exactly as in setup 2.

2.5.2 Control setup without stimulation for NETosis

In this control setup, neutrophils were not stimulated to undergo NETosis. All steps and timepoints were performed exactly as in setup 2. Instead of PMA, LCNM was used. Neutrophil integrity was checked before and after the experiment.

2.6 Time-lapse analysis

All results were blinded before analysis. In order to quantify the change of chromatin expansion during the process of NETosis in neutrophils, which corresponds to the change in chromatin area in 2D microscopy, an image segmentation script was used. It was developed by our research group and recently published (Neubert et al. 2018). The script was run on the software Matlab (v. 2014a). The algorithm analyzed single cells out of live cell images that were created by wide field fluorescence microscopy. These cells were projected as 2D objects, and the projected chromatin area of single cells was quantified. For single cells, high contrast areas were carved out, smoothed, and filled in order to produce an outline image that could be analyzed. To reduce problems deriving from different staining intensities or background fluctuations, total intensity values were normalized. The generated data was plotted on an area-time curve. From these curves two characteristic time points were chosen as previously demonstrated by our group (Neubert et al. 2018): t1 and t3. t1 is defined as start of NETosis phase P2: start of first chromatin area increase. t3 is defined as start of P3: second start of increase in chromatin area. Neutrophils that did not show two distinct time points were counted only for t1 if clearly distinguishable.

These timepoints divide the process of NETosis into three distinct phases: P1, P2 and P3, as described above. P1 (t0 to t1) describes the activation-phase. P2 (t1 to t3) describes the swelling phase. P3 (from t3 onwards) describes the rupture of the cell and release of NETs. Quantitative membrane and chromatin analysis were performed using the same segmentation procedure. Each cell's image-stack was split into a grid of 15 x 15 pixel sized sub-windows. Measuring the average increase or decrease of chromatin area per window generated a growth/shrink vector for each of these segments. Averaging all frame vectors of a respective segment resulted in the final vector plot.

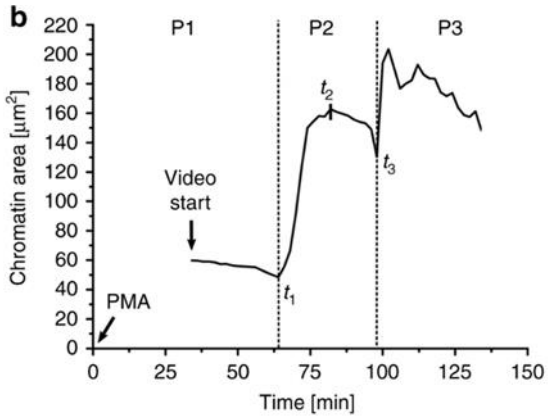

Fig. 6: Corresponding chromatin area of a NETotic neutrophil as a function of time. From Neubert and Meyer et al. "Corresponding chromatin area of a NETotic neutrophil as a function of time reveals three distinct phases. P1: Activation, lobulated nucleus. P2: Decondensation/expansion of chromatin within the cell (t_1 = start of chromatin expansion, t_2 = maximal chromatin expansion within the cell); cell rounding. P3: Rupture of the cell membrane and NET release (t_3 = NET release)." (Neubert et al. 2018), (edit: cropped from original, license: CC BY 4.0)

In addition to digital analysis, the image-stacks were analyzed by the naked eye. Characteristic changes of nucleus morphology and size were identified and categorized into the different phases of NETosis. Cross-checking results with the computational analysis by the algorithm was performed regularly.

2.7 Stimulation of NETosis with 0.2% methylcellulose

In the process of adjusting the cell medium, some experiments showed unspecific activation of neutrophils before a stimulus was added. This experiment was designed to test whether methylcellulose, an ingredient to increase medium viscosity to a blood-like level, induces NETosis.

50 000 isolated human neutrophils each were resuspended in either 400 µl perfusion medium (suspension A) or 400 µl perfusion medium without methylcellulose (suspension B). Three times 100 µl of suspension A and three times 100 µl of suspension B were plated into a 96-well-plate (clear bottom, Merck). The plate was incubated for 30 minutes at 37°C and 5% CO_2. The neutrophils were viewed under an inverted microscope after incubation. Afterwards, the cells were incubated for 30 minutes more and viewed again.

3 Results

3.1 Donors and cells

Neutrophils were isolated from healthy donors and analyzed under different conditions. Tab. 3 displays the distribution for all experiments.

Tab. 3: Number of neutrophils analyzed for each experiment.

Condition	Donor		
	A	**B**	**C**
Control (no flow)	60	70	90
Flow-pretreatment (6.5 Pa)	60	70	90
Continuous flow (0.1 Pa)	60	70	90
Continuous flow (0.5 Pa)	60	70	90
	∑ 240	∑ 280	∑ 360

As an example: In the condition "Control (no flow)" 60 neutrophils from donor A were analyzed, 70 from donor B and 90 from donor C in a single experiment per donor. The total number of neutrophils analyzed per donor was 240 for donor A, 280 for donor B and 360 for donor C.

3.2 Live cell imaging

Neutrophils exposed to either continuous shear stress or shear stress pre-treatment showed an altered process of NETosis in comparison to the control. Figure 7 shows the results of all four conditions for each donor individually. Especially neutrophils of donor B showed very distinct differences in the phases of NETosis. In comparison to the control phase, P1 was prolonged in all three shear stress conditions while phase P2 was shortened under continuous flow. Looking at the total duration of NETosis, the same effect as in P1 was observed. A similar effect was seen in donor C. Neutrophils showed a prolonged phase P1 and a shortened phase P2 under continuous shear stress conditions. This effect was not clearly visible in donor A. Although neutrophils that had been continuously exposed to 0.1 Pa shear stress showed a prolonged phase P1 and a shortened phase P2, this could not be observed at 0.5 Pa. In this condition, the standard deviation was very high and many cells were washed away before entering phase P2.

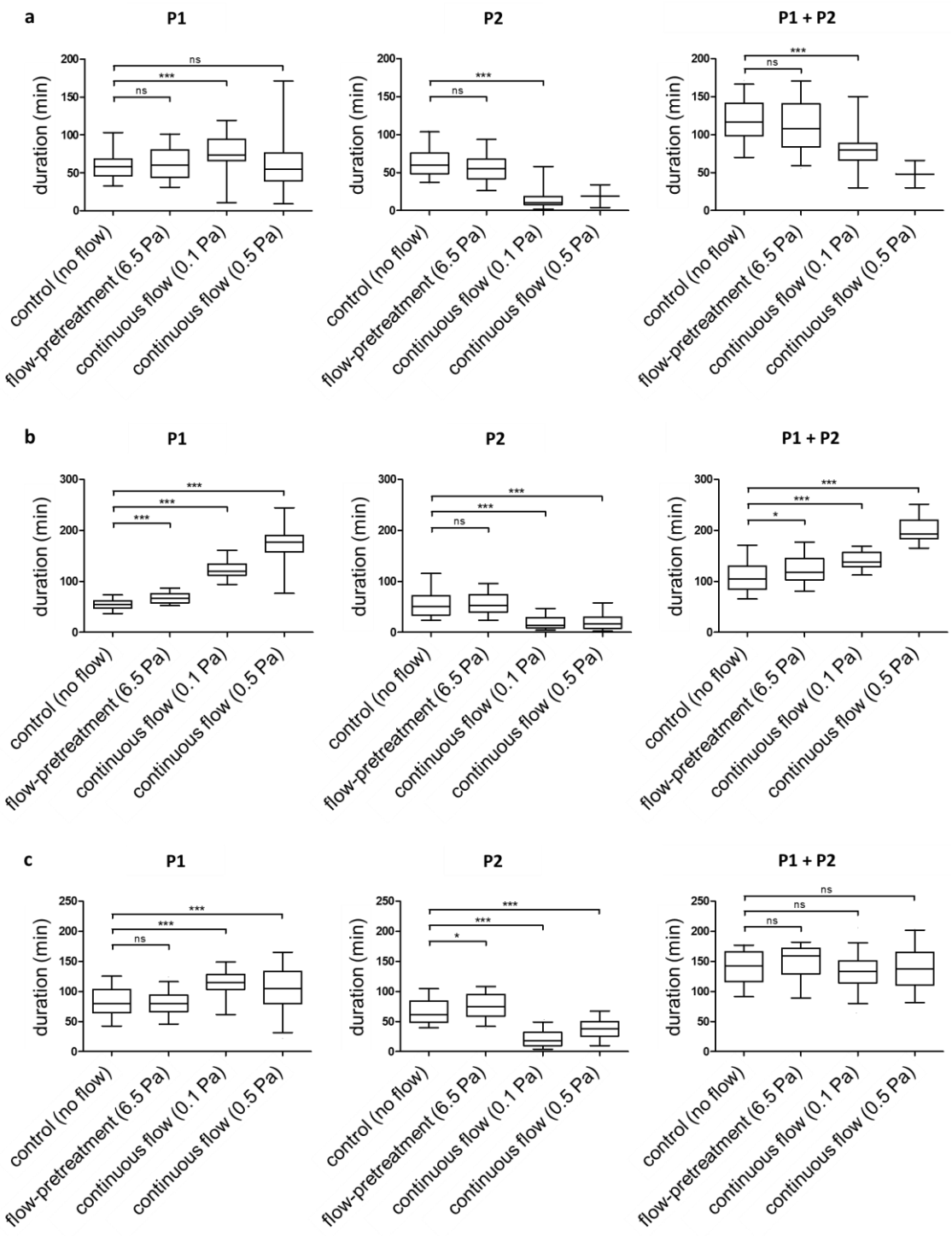

Fig. 7: Data from life cell imaging. Comparison of NETosis phases P1, P2 and total duration of NETosis (P1 + P2) under different flow conditions in comparison to the control without flow for three different donors: **a.)** Donor A. **b.)** Donor B. **c.)** Donor C. NETosis phase P1 is prolonged or unchanged under flow conditions in comparison to the control in all three donors. In donor B prolongation of P1 correlates positively with increased shear stress. NETosis phase P2 is shortened in continuous flow in all three donors while it is unchanged or prolonged under flow-pretreatment in comparison to the control. Total duration of NETosis in comparison to the control shows mixed results for each donor. Statistics: Mann-Whitney test, two tailed with confidence intervals at 95%, *$p < 0.05$; **$p < 0.01$; ***$p < 0.001$; ns = not significant. Boxplots display 25th and 75th percentile. The horizontal line displays the median. Whiskers represent SD. n = 240 cells for donor A, n = 280 cells for donor B, n = 360 cells for donor C.

3.2.1 **Image sequences**

The experiments were captured with an inverted fluorescent microscope, creating videos with one image per minute. Stained neutrophil nuclei presented in polymorphic shapes and changed during NETosis as described. Figure 8 shows a representative nucleus at the indicated time points t1 and t3.

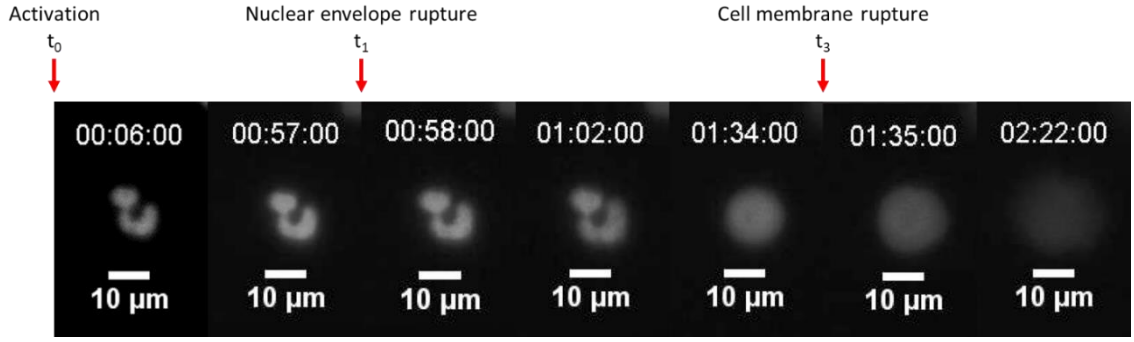

Fig. 8: Nucleus of a representative neutrophil undergoing NETosis without any application of shear stress. The timescale shows hh:mm:ss. Activation with PMA happened at t_0.

3.2.2 **Graphical analysis**

The videos were analyzed and plotted on an area-time-curve. Neutrophils that had not been exposed to shear stress showed chromatin expansion profiles in line with published data (Fig. 9a+b). Neutrophils that had been exposed to shear stress, especially under continuous flow conditions, showed late time points t1 with a rapid expansion of chromatin and a shortened duration between t1 and t3 (Fig. 9c). While in the experiments with flow pre-treatment or no flow most timepoints were clearly distinguishable, in the continuous flow setup distinct timepoints, especially t3, could only be identified for a fraction of all NETotic neutrophils. In the majority of neutrophils, timepoint t1 was clearly visible, marking the start of chromatin expansion, while t3 was not detectable within the given timeframe of 240 minutes (Fig. 9d). This discrepancy was even greater when continuous shear stress with 0.5 Pa was applied. In the continuous flow experiments, some cells could not be analyzed since they were washed off before entering NETosis phase P2. In 0.1 Pa continuous shear stress experiments the proportion of such cells was estimated below 5% of all cells analyzed, while in 0.5 Pa continuous shear stress experiments it was estimated below 10% with one experiment standing out showing over 50% of cells being washed off before entering NETosis phase P2.

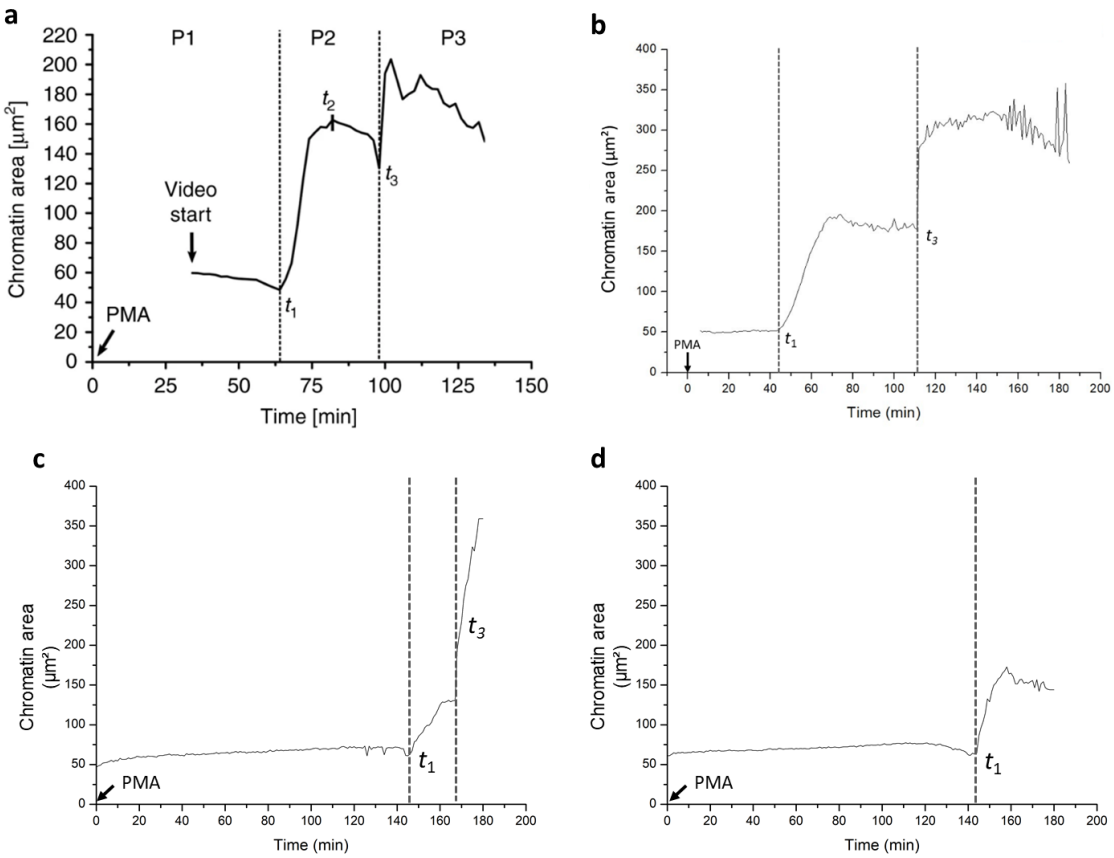

Fig. 9: Area-time-curves of representative neutrophils under different conditions.
a.) Reference neutrophil from Neubert and Meyer et al. (Neubert et al. 2018), (edit: cropped from original, license: CC BY 4.0). **b.)** Representative neutrophil from control experiment showing similar results as in a. **c.)** Neutrophil undergoing NETosis under continuous shear stress of 0.1 Pa with late distinct timepoints t1 and t3, longer phase P1 and shorter phase P2. **d.)** Neutrophil undergoing NETosis under continuous shear stress of 0.1 Pa showing only t1 without further expansion of chromatin thereafter.

3.3 Buffer modalities

3.3.1 Acidic medium promoted better adhesion of neutrophils

Different results for neutrophil adhesion are shown in Figure 10. Phosphate-buffered saline (PBS)-buffered medium showed poor neutrophil adhesion. This is very likely due to the less potent buffering properties of PBS resulting in a non-acidic pH. In comparison, both HEPES-buffered media showed much more adherent neutrophils. Differences between RPMI + PBS and HBSS + PBS could not be observed. RPMI + HEPES showed slightly fewer adherent neutrophils than HBSS + HEPES. After the experiment, the different media were tested with a pH-strip showing differences ranking from pH = 7.0 – 7.8.

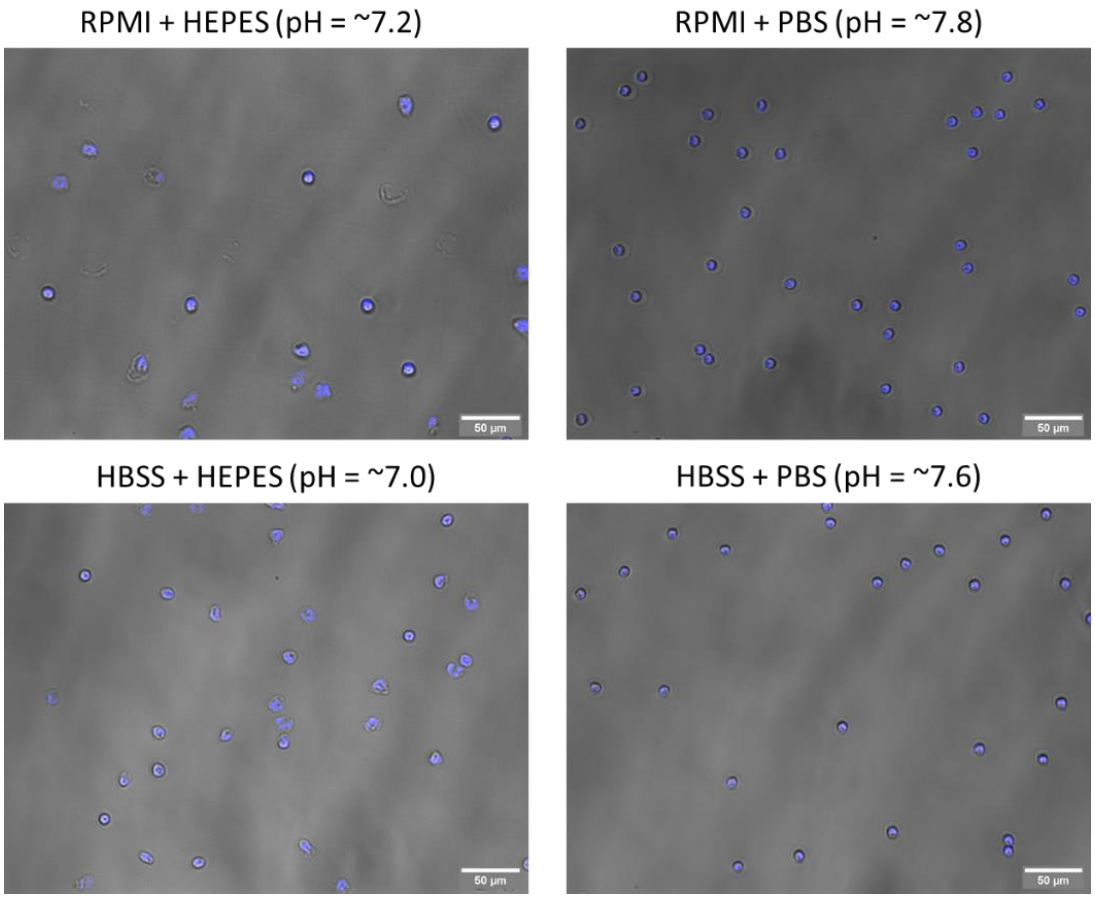

Fig. 10: Representative images of neutrophils adhering in different media. The nucleus was stained with HOECHST (blue). Cell bodies were viewed under light microscopy. Non-adherent neutrophils show a round shaped cell body with high contrast cell membrane and a dense, small nucleus due to a spherical geometry and a high volume/surface ratio. Adherent neutrophils show polymorphous cell bodies with larger cell area, a low contrast cell membrane and a less dense, larger nucleus as a result of a flattened geometry and a lower volume/surface ratio, as described elsewhere (Brinkmann et al. 2012). The images show no adherent neutrophils in conditions with PBS. In conditions with HEPES adherence was better with HBSS and lower pH.

3.3.2 **Neutrophils in LCNM buffer showed good adhesion and vitality**

As a consequence of these findings, another buffer (LCNM) was composed to meet the required conditions. The buffer contained HBSS +/+ (see Tab. 1) and FCS to provide all essential nutritional supplements and prevent spontaneous NETosis. The pH was titrated to 7.2 to ensure optimal cell adhesion and the buffer was sterile filtrated to prevent contamination.

Neutrophils seeded into a flow chamber and incubated in LCNM for 30 minutes at 37°C and 5% CO_2 showed very good adhesive properties and vitality. After one experiment following setup 2, the pH was measured with a pH-strip at pH ~ 7.2.

3.3.3 **0.2 % Methylcellulose induced NETosis**

Resuspending neutrophils in medium with 0.2 % methylcellulose showed a high degree of NETosis after one hour in comparison to neutrophils in medium without.

After 30 minutes of incubating neutrophils in medium with and without methylcellulose, cells were analyzed under an inverted microscope. In both conditions, neutrophils showed no visible signs of NETosis. After 30 more minutes of incubation, neutrophils were re-examined. The condition with methylcellulose showed approximately 50 % NETs of all visible neutrophil nuclei, while the condition without methylcellulose showed no NETs at all. A quantification by the naked eye by two independent observers confirmed this finding.

4 Discussion

The aim of this study was to investigate whether fluid shear stress influences the process of NETosis in human neutrophils. Evidence that shear stress seems to have an effect on NETosis in general has been presented (Yu et al. 2018). We hypothesized that shear stress has different effects on the process of NETosis depending on the phase the neutrophil is currently in. To investigate this effect, live cell imaging setups with application of flow and stimulation for NETosis were used, enabling a detailed analysis of the different phases of NETosis in individual cells with and without application of shear stress.

4.1 The influence of shear stress on NETosis

The results showed clear differences in two donors in the overall duration of NETosis in neutrophils exposed to shear stress in comparison to the control. Neutrophils that have been pre-treated with shear stress showed a prolonged phase P1 (Figure 7). This effect was even stronger in neutrophils exposed to continuous shear stress, while P2 was shorter under this condition. These findings indicate that shear stress alters the process of NETosis. In the following, different models about the underlying mechanism of the observed effect are discussed.

4.2 Cytoskeletal changes induced by shear stress alter the duration of NETosis phases P1 and P2

Early studies have shown that shear stress has a stimulating effect on the cytoskeleton of neutrophils (Okuyama et al. 1996). The cytoskeleton also plays an important role in NETosis. Recent work showed that actin is degraded during NETosis (Neubert et al. 2018). Another group supported these findings by showing similar observations. In addition, they conducted an experiment where degradation of actin was inhibited resulting in fewer neutrophils undergoing NETosis (Thiam et al. 2020). Both findings lead to the possible explanation that shear stress stimulates neutrophils to strengthen their cytoskeleton and thereby delaying its degradation. Since the degradation process takes place in phase P1 of NETosis, this explanation would be in line with the results of this study. Experiments performed with red blood cells have shown that impaired integrity of cellular mechanics lead to a higher sensitivity to shear-stress-related cell rupture (Horobin et al. 2019). Presuming a similar mechanism in neutrophils, the degradation of the cytoskeleton may lead to a higher vulnerability to external mechanical forces. Under continuous flow conditions, such forces were constantly applied and possibly led to a shortened phase P2 and an earlier rupture of the cell membrane. This hypothesis is supported by the fact that in NETotic neutrophils under static conditions P2 remained unchanged even in neutrophils that had been pre-treated with shear stress. The observation of many neutrophils under continuous flow being washed-off around the timepoint t1 indicated that these neutrophils showed impaired adhesion,

which is another sign for a disintegrated cytoskeleton since adhesion is strongly dependent on it (Hohmann and Dehghani 2019). Similarly, the majority of neutrophils under continuous flow seemed to have started phase P2 but did not show the characteristic spread of chromatin inside the cell. These cells lacked a clearly visible rupture of the cell membrane at timepoint t3. The chromatin started a swelling process but kept its nucleus-like shape. This observation indicates that in these cells timepoints t1 and t3 happened simultaneously or nearly simultaneously, meaning the rupture of the cell membrane followed the rupture of the nuclear envelope immediately. Further investigation of the NETs of these neutrophils may help understanding this process. While these observations suggest a strong link between the differences in NETosis phases and the cytoskeleton, more research is required in this field. In order to investigate the role of actin throughout the process of NETosis under shear stress and without, similar experiments could be performed with an actin live staining. Many suitable staining procedures are available for example the SiR-actin kit (Spirochrome, Stein am Rhein, Switzerland). An experimental setup could be established in which neutrophils are isolated and seeded into a flow chamber like in this study. In addition to or instead of DNA-staining with HOECHST, neutrophils could be treated with SiR-actin. Thereafter, the flow chamber is installed into a suitable fluorescent microscope for live cell imaging. This setup would allow a flexible application of flow like in this study. However, it is important to determine the optimal SiR-actin concentration to maintain a balance between sufficient signal strength to properly visualize the cytoskeleton and short incubation time and concentration to prevent cellular toxicity. This setup would allow a live analysis of the cytoskeleton under static and flow conditions. Comparing static and flow conditions of DNA-stained and actin-stained neutrophils could lead to a deeper understanding of the role of cytoskeletal changes during NETosis and under shear stress.

4.3 Shear stress promotes intracellular calcium-influx - a potential trigger for NETosis

Recent research using eosinophil granulocytes revealed that shear stress influences the cytoskeleton and calcium regulation of these cells. Eosinophils that had been under shear stress (2-4 Pa) showed a strong calcium influx after less than five minutes of perfusion followed by changes in the f-actin cytoskeleton which led to a flattening of the cells and the development of pseudopods (Son et al. 2020). In neutrophils it has been shown that shear stress regulates intracellular calcium flux *via* a complex of LFA-1/ICAM-1/Kindlin-3. Release of calcium from the endoplasmatic reticulum into the cytoplasm as well as extracellular calcium influx mediated *via* Orai1 increase cytosolic calcium concentration under higher shear stress conditions (Immler et al. 2018). It has also been shown that calcium-influx leads to NETosis in neutrophils (Douda et al. 2015). These data suggest that shear stress induces or contributes to NETosis via increased calcium influx. However, the same group found that PMA induced NETosis was abundant even in absence of extracellular

calcium, suggesting a different NETosis pathway that is either calcium-independent or relies on intracellular calcium flux. Since the regulation of calcium homeostasis is very complex, isolated findings on how calcium flux influences NETosis have to be interpreted with caution.

4.4 Shear stress influences neutrophils through mechanotransduction

Mechanotransduction plays a major role in the function of neutrophils under physiological conditions. They have the capability to adapt their reactivity to certain stimuli under the influence of shear stress (Mitchell and King 2012; Mitchell et al. 2014), and they can alter their response in a stimulus-dependent manner. This suggests a well-balanced system in which neutrophils under shear stress optimize their activity to certain stimuli such as platelet-activating factor (PAF) and adapt to their environment (Mitchell et al. 2014). However, most mechanisms by which shear stress influences the metabolism of neutrophils remain poorly understood. Previous investigations have shown that cell adhesion molecules are associated with a direct activation of molecular pathways including cyclic guanosine monophosphate (cGMP) inside the neutrophil (Ekpenyong et al. 2015). When neutrophils bound to E-selectin/CD62E were exposed to fluid shear stress they showed a strong upregulation of CD11b/CD18 and phosphorylation of MAPK p38 (Hentzen et al. 2002). The latter is a key player in the PMA-stimulated NETosis pathway. PMA stimulates neutrophils by activating PKC which in turn activates NADPH oxidase. As a result, superoxide anions are produced, driving NETosis through activation of MPO and NE. This process has been found to be MAPK p38-dependent with one group working with neutrophils from mice postulating MAPK p38 being activated by superoxide anions (Saito et al. 2005) and another group describing MAPK to be essential for activation of NADPH-oxidase in tumor necrosis factor alpha (TNF-α) activated neutrophils (Dang et al. 2006). The prolonged NETosis demonstrated in the present study seems to contradict these findings by which shear stress has an activating effect on the NETosis pathway under PMA-stimulation. It is important to mention that neutrophils in our experiments did not bind to any specific target but adhered to an unspecific adhesive hydrophilic polymer surface. To investigate the role of mechanotransduction, further experiments are needed in which neutrophils bind to specific targets. A potential candidate would be E-selectin/CD62E, which is expressed on endothelial cells in response to LPS or inflammatory cytokines like TNFα or interleukin-1β (IL-1β). It is crucial for tethering, rolling, arrest and transendothelial migration of neutrophils by binding to glycosylated ligands on neutrophils like PSGL-1 and E-selectin ligand-1 (ESL-1) (Lawrence et al. 1994; Huang et al. 2021). Recent studies even suggest a regulatory effect of E-selectin/CD62E-clustering in the process of transendothelial migration (Huang et al. 2021). Another interesting candidate for flow experiments is ICAM-1/CD54. This protein is essential for facilitating strong adhesion between neutrophils and endothelial cells by binding to lymphocyte function-associated antigen 1 (LFA-1), which is required for

transendothelial migration (Lyck and Enzmann 2015). To investigate the extent by which mechanotransduction influences NETosis, an experimental setup like the one used in the present study could be established with flow chambers coated with ICAM-1/CD54 or E-selectin/CD62E. This would improve the setup to mimic a more physiological environment and different coatings can be compared. However, the influence of mechanotransduction itself on NETosis cannot be studied in an isolated fashion. Since shear stress can only be applied to adherent neutrophils an experimental setup in which adherent neutrophils are exposed to shear stress without potentially triggering mechanotransduction needs to be developed.

4.5 Neutrophils under flow are less exposed to ROS released from neighboring NETotic cells

An important factor that needs to be addressed is the release of ROS by activated neutrophils. Neutrophils that have been stimulated with PMA are activated through a pathway involving NADPH oxidase and the production of ROS. After being produced, ROS passively diffuse intra- and extracellularly. Hydrogen peroxide is a potent inducer of NETosis (Fuchs et al. 2007). Neutrophils near a NETotic neutrophil might be exposed to ROS and stimulated for NETosis. In stimulation experiments this would lead to cumulative stimulation of NETosis through ROS exposure in addition to the applied stimulant, possibly resulting in a faster onset. This effect, however, can only occur sufficiently under static conditions since ROS are rapidly rinsed off under flow. This observation can provide another explanation how fluid shear stress influences the duration of NETosis. The lack of co-stimulation by ROS production of neighboring cells under continuous flow might lead to a slower activation phase P1 in comparison to static conditions. However, it does not explain the differences between static conditions with and without flow pre-treatment leading to the assumption that at least another effect must play a role in this mechanism.

4.6 Comparing continuous flow with flow pre-treatment

To investigate neutrophils under fluid shear stress, two experimental setups were established. The concept of continuous flow applied to cells in flow-chambers is widely used and certainly offers several advantages. In live cell imaging, it is particularly useful to identify changes in the cells for example in a NETotic neutrophil under flow. This system is an approach to mimic intravasal conditions *in vitro*. Pharmacological compounds such as stimulators for NETosis are added to the cells in a flowing environment reflecting the intravasal conditions much better than in a static experiment. Another approach to explore the effect of shear stress on neutrophils was to pre-treat the cells with shear stress prior to stimulation for NETosis. With this setup using a syringe-pump, a cost-effective alternative was established. While the setup was limited by the volume of the syringes, other advantages showed the

usability of this procedure. The temperature could easily be changed by storing the syringes in a heated water bath. During the imaging sequence the temperature remained the same as in the control experiments. For other applications, the setup offers great flexibility on timing, duration and intensity of applied shear stress and composition of the perfusion medium. Additional pump units can be connected and synchronized to form a scalable setup. When focusing on underlying mechanics, this setup offers several advantages in exploring mechanistic and pharmacological aspects without the need of a complex physiological environment. Furthermore, this setup allows to test a large sample size of up to 90 neutrophils per experiment. These cells can be analyzed in detail by creating video clips for each cell individually, providing data that can be analyzed using different methods following the investigators demands. This enables a valid comparison between different conditions in one donor. However, the experimental implementation is complex and not many donors could be tested at the same time.

4.7 Using methylcellulose in flow chamber experiments

Methylcellulose is a common ingredient in cell media to mimic blood viscosity. However, only few investigations addressed a potential activating effect on cells. The observation that methylcellulose is a potent inducer of NETosis corresponds to findings from over three decades ago where it was shown that it activates neutrophils to release neutrophil elastase (Jackson et al. 1989). The interaction of methylcellulose with neutrophils and other human leucocytes should therefore be considered when planning the experimental setup. Interestingly, dextran, another commonly used ingredient to increase media viscosity has been reported to have a modulating effect on human endothelial cells (Rouleau et al. 2010). Adding substances to increase media viscosity can therefore cause a potential risk of confounding cell activation. As an alternative, the concept of non-dimensionalization avoids additives in flow experiments by increasing shear stress with an elevated flow rate instead of viscosity. However, this would require a significantly higher flow rate which might not be applicable to all experimental setups due to limitations in device geometry or reservoir volume.

4.8 Limitations of the experiments

Viscosity and shear stress had been calculated using a specific formula (Eq. 1). In order to calculate the shear stress applied to adherent neutrophils in the flow chamber, variables like cell size and cell geometry were neglected and Δh assumed to be as small as possible. This approximation enabled a precise setup of different shear stress modalities to investigate the mechanistic effect on neutrophils. When translating these findings into *in vivo* experiments or creating a more physiological *in vitro* setup, parameters such as turbulent flow on the surface of cells and the physical properties of blood as a non-Newtonian fluid need to be

considered. To standardize shear stress in *in vitro* experiments a laminar flow is typically applied. Since in the human body neutrophils are exposed to both, laminar and turbulent flow, this setup only partly represents physiological conditions. A hybrid model exposing neutrophils to laminar as well as turbulent flow would be an interesting approach. To generate turbulent flow conditions in *in vitro* experiments requires a much more complicated architecture of flow devices and analytical tools, which might explain why such experiments are rarely employed. Another important factor to consider in flow experiments is that blood can be estimated to act as Newtonian fluid, but the physiological behavior of blood as non-Newtonian fluid is more complex (Liu et al. 2021). Since a Newtonian fluid is required to calculate shear stress with commonly used formulas, most standard *in vitro* cell media, which are Newtonian fluids, cannot substitute whole blood. This bias can be avoided by perfusing with whole blood instead of medium as shown in some investigations (Yu et al. 2018; Chiang et al. 2022). However, using whole blood introduces a significantly more complex variable into *in vitro* experiments, for example by the use of anti-coagulants.

As a pilot study on mechanistic aspects of NETosis this study was designed using an experimental setup to explore key processes of NETosis under shear stress conditions. The setup provided many advantages and high sample sizes in comparing different conditions for one donor. However, the complex setting limited processing of many different donors at the same time.

Using only the naked eye to capture the described time points during NETosis yielded surprisingly accurate results. By cross-checking with data generated by computational analysis the differences were negligible.

The validation of manual analysis versus computational analysis and fully automated solutions has been described by many studies (Hirneiss et al. 2007; Giegold et al. 2009; Jonuscheit et al. 2011; Brullmann et al. 2012). Results depended heavily on the investigated system's complexity and the quality of employed software. While one study showed significant benefits of fully automated chemotaxis analysis for *in vitro* experiments with neutrophils rolling on endothelial cells in flow chambers compared to manual analysis related to precision and time-efficiancy (Giegold et al. 2009), another study evaluated a fully automated solution for measuring corneal endothelial cell density as insufficient and manual analysis was recommended (Miyagi et al. 2020).

For the present study requirements for computational analysis or even fully automated solutions were relatively complex. In comparison to the above-mentioned examples, a dynamic process with two-dimensional changes of highly complex shapes for individual cells and great differences between each cell requires a sophisticated software solution. With the given resources the algorithm developed proved to be sufficient for analyzing less complex shaped nuclei and yielded additional data sets on DNA area changes that were used to compare the results with manual analysis and reference studies (Neubert et al. 2018). However, manual analysis proved to be more accurate in capturing time points of cells that

showed a complex shaped polymorphic nucleus with small plasma bridges. In some cases, such polymorphic nuclei were not recognized by the algorithm. In terms of time-efficiency manual analysis was performed nearly two times faster than computational analysis. This method was used in the experimental setup. To prevent interindividual bias leading to extensive standard deviation in other studies (Giegold et al. 2009), one investigator was chosen to perform all manual analyses. In addition, blinding of raw data was essential to prevent expectation bias by the investigator.

Using LCNM medium enabled live cell imaging under flow and promoted neutrophil adhesion and viability. However, LCNM as a very minimalistic medium does not represent complex whole-media or even blood. It proved to be very useful in investigating mechanistic effects without confounding by unnecessary ingredients or the aforementioned light effect. In order to translate these findings into more complex physiological setups, buffer composition needs to be adjusted accordingly.

4.9 Physiological and pathophysiological relevance

The results of this study show that shear stress has a modulating effect on NETosis depending on the phase of the NETotic neutrophil. This finding introduces a new variable influencing neutrophils aside from biochemical stimulation by soluble mediators. Biophysical properties like shear stress seem to play an important role in the regulation of NETosis. Considering environmental factors neutrophils are exposed to is crucial to understand the (patho-)physiological relevance of these findings. In the vascular system, neutrophils flow either in the central pool or attach to blood vessel walls and roll in the marginal pool. The amount of shear stress neutrophils are exposed to depends on different modalities like flow rate, viscosity of the blood, vessel diameter and neutrophil shape, size and position. Vessel diameter is regulated by vascular smooth muscle cells (VSMCs). These cells surround blood vessel walls, providing stability, shape and by contracting and relaxing, regulate diameter and flow (Metz et al. 2012). As mentioned before, shear stress in the microvascular system ranges from 0.3 to 9.5 Pa with higher values in smaller vessels. However, in some diseases this complex regulation of vessel diameter is altered, like in atherosclerosis (Boesen et al. 2015). In such diseases neutrophils are likely to be exposed to higher shear stress in comparison to physiological conditions and stimulated to undergo NETosis for example by cholesterol crystals (Warnatsch et al. 2015). In contrast, peripheral tissue hypoxia leads to a local capillary dilatation. Another disease that is relevant to neutrophils and shear stress is thrombosis. In thrombotic lesions neutrophils can get trapped and are exposed to turbulent blood flow and high shear stress (Yu et al. 2018). Neutrophils in thrombi are interacting with platelets, which can lead to a higher rate of NETosis and a higher inflammatory response, accelerating the pathogenesis (Caillon et al. 2022). Neutrophil-platelet interaction in an environment where neutrophils are exposed to shear stress also plays a crucial role in the pathogenesis of acute lung injury (Caudrillier et al. 2012; Surolia et al. 2021). In a study performed in mice with

ventilation induced lung injury, platelet-neutrophil interaction presented as defining factor for the abundance of NETs and severity of symptoms. With platelet depletion, the inflammatory response was significantly lower in comparison to normal platelet counts (Rossaint et al. 2014). Neutrophils bind through the heterodimeric integrin $\alpha_M\beta_2$ (CD11b/CD18), also referred to as macrophage-1 antigen (Mac-1) or complement receptor 3 (CR3), to glycoprotein (GP) Ibα on platelets' plasma membrane (Simon et al. 2000). Blocking CD11b/CD18 with a monoclonal antibody had a similar effect as platelet depletion suggesting this receptor to mediate neutrophil stimulation (Rossaint et al. 2014). Neutrophils and other innate immune cells like macrophages with altered CD11b as a result of gene-polymorphisms in the ITGAM-gene showed impaired adhesion and immune function (Hom et al. 2008; Rhodes et al. 2012; Khan et al. 2018).

Another disease that needs to be considered is hypertension. In high blood pressure, neutrophils are constantly exposed to high shear stress. The effect of such environmental conditions has been investigated with *in vitro* experiments and a rat model called spontaneous hypertensive rat (SHR). It has been shown that neutrophils and HL60 cells sensed shear stress mainly through the formyl peptide receptor (FPR). In vital cells with intact FPR a formation of membrane protuberances termed pseudopods was observed, which, in contact with shear stress, were retracted. Absence or dysfunction of this receptor led to a decreased projection of pseudopods and, under shear stress, to a decrease in retraction (Makino et al. 2006). In SHRs a significantly lower concentration of FPR was measured on neutrophils in comparison to wild type rats. These neutrophils showed the same inability to react to shear stress. It was hypothesized that hypertension stimulated an upregulation of matrix metalloproteinases, which are associated with cleavage of leucocyte membrane proteins and as a consequence led to cleavage of FPR. SHRs treated with doxycycline, a matrix metalloproteinase inhibitor, produced neutrophils that showed a higher concentration of FPR and recovered pseudopod reactivity (Chen et al. 2010). These findings suggest a strong link between chronic hypertension and reduced reactivity of neutrophils to shear stress. While in the present study neutrophils were isolated from healthy donors, it should be considered to repeat such experiments with neutrophils from patients with chronic hypertension. Adding matrix metalloproteinases or an inhibitor *in vitro* would help to explore whether these findings in SHRs can be applied to human cells, too, and investigate the effect on NETosis.

A topic that is equally interesting in this context is smoking. Several studies have shown that nicotine and tobacco smoke are potential activators of neutrophils and even induce NETosis or aggravate PMA induced NETosis (Lee et al. 2017; Qiu et al. 2017; Omer-Cihangir et al. 2021). However, other studies seem to contradict these findings, proposing an inhibiting effect on NETosis and thereby a reduced immune function (Bokaba et al. 2017; Reidel et al. 2018; Corriden et al. 2020). Further studies are needed to investigate the discrepancy between these observations. However, smoking seems to have a strong effect on NETosis. It would be interesting to conduct similar experiments as in the present study with neutrophils from

smokers in comparison to non-smokers to see whether shear stress has a distinct effect on NETosis in this context. This might give insight into the pathology of atherosclerosis, to which smoking is one of the most important risk factors.

Another important variable that needs to be considered is temperature. Since NETosis is partly an enzyme independent swelling process it is likely to happen faster with higher temperature. In *in vitro* experiments short-term fever-range hyperthermia increased the number of NETs at two hours after stimulation with PMA (Keitelman et al. 2019). It is therefore very important to ensure a constant temperature during in vitro live cell experiments by using devices like heating chambers.

4.10 Outlook

The present study serves as a pilot project on the mechanistic aspects of NETosis under the influence of different pathologies and physical aspects like shear stress. It was shown that NETosis is influenced by shear stress in different donors. The effect was investigated in detail for each phase of NETosis. The findings suggest a modulating effect of shear stress on NETosis. To understand the underlying mechanisms of the observed effect, further experiments need to be conducted. The setup from the present study offers many ways to easily adapt parameters like stimuli, coatings, shear stress and stainings to extend experimental conditions on demand. Promising approaches would include using different NETosis stimuli like LPS, calcium ionophore or complement factor 5a, as well as using coated flow chambers with for example E-selectin/CD62E or ICAM-1/CD54 or with human endothelial cells. Blocking such surface molecules could help to understand the role of mechanotransduction. Considering the role of cytoskeletal changes during NETosis, a live cell actin staining as described above can be used to elucidate the involvement of actin in this process. Another promising approach involves the use of neutrophils from donors with certain diseases and/or risk factors like hypertension and smoking. As discussed above, such neutrophils react differently to shear stress in comparison to those from healthy donors. Conducting NETosis experiments under shear stress could therefor help to understand the pathophysiological relevance in this context.

5 Summary

Neutrophil granulocytes, the most abundant type of circulating immune cells, engage in a process called NETosis when encountering certain pathogens and danger signals or experimentally induced by phorbol-12-myristate-13-acetate (PMA). During NETosis the chromatin decondenses and through a passive swelling process this leads to the rupture of the nuclear and subsequently of the plasma membrane. A meshwork of desoxyribonucleic acid (DNA) decorated with nuclear and cytosolic proteins is released into the extracellular space forming Neutrophil Extracellular Traps (NETs). It has been shown that this process can be divided into two distinct phases. The first phase, being energy-dependent, starts at stimulation and ends at chromatin decondensation. The second phase consists of a passive swelling process ending at the rupture of the plasma membrane and the release of the NET. There is experimental evidence that fluidic shear stress generated by the bloodstream to adherent neutrophils attached to the vessel's wall is promoting NETosis. The underlying mechanism, however, remains unknown.

The aim of this study was to establish an experimental setup and to investigate the effect of fluidic shear stress on adherent neutrophils undergoing NETosis in greater detail focusing on changes of the different phases of NETosis. All experiments were performed with human neutrophils and analyzed by live cell imaging. For this purpose, a novel cell culture medium was developed to avoid unspecific cellular activation and provide optimal cell adherence and survival. Fluid chambers and cell dishes, two different pump systems for flow application, a DNA live stain to visualize chromatin, and PMA as a stimulus for NETosis were used. With a circular pump continuous shear stress was generated and with a syringe-pump neutrophils were pre-treated with shear stress before stimulation. Videos obtained by live cell imaging were analyzed either by computational analysis or by the naked eye.

The setup proved to be suitable for investigating NETosis under shear stress. All variables such as staining, stimuli, and shear stress quality and quantity could be modified. Analysis of live cell imaging allowed to clearly characterize distinct elements of NETosis.

The results of the investigation showed that neutrophils exposed to either continuous shear stress or shear stress pre-treatment underwent an altered process of NETosis in some donors in comparison to cells that were not exposed to shear stress. The most common observation was that neutrophils treated with shear stress during or before undergoing NETosis showed a prolonged first phase until the swelling of chromatin. Under continuous shear stress a shortened second phase until the rupture of the plasma membrane was observed. These findings indicate that shear stress did influence NETosis, altering the duration of its phases. Previous studies suggested a link between shear stress and cytoskeletal changes, calcium-homeostasis, or mechanotransduction. The development of the methodology employed in this work by creating different experimental setups offers the possibility to further investigate the molecular mechanisms behind NETosis under the influence of shear stress adapted to experimental needs.

6 References

Abram CL, Lowell CA (2007): Convergence of immunoreceptor and integrin signaling. Immunol Rev 218, 29-44

Aratani Y (2018): Myeloperoxidase: Its role for host defense, inflammation, and neutrophil function. Arch Biochem Biophys 640, 47-52

Barnes BJ, Adrover JM, Baxter-Stoltzfus A, Borczuk A, Cools-Lartigue J, Crawford JM, Daßler-Plenker J, Guerci P, Huynh C, Knight JS et al. (2020): Targeting potential drivers of COVID-19: Neutrophil extracellular traps. J Exp Med 217

Beck M, Hurt E (2017): The nuclear pore complex: understanding its function through structural insight. Nat Rev Mol Cell Biol 18, 73-89

Bedouhène S, Dang PM, Hurtado-Nedelec M, El-Benna J (2020): Neutrophil Degranulation of Azurophil and Specific Granules. Methods Mol Biol 2087, 215-222

Boesen ME, Singh D, Menon BK, Frayne R (2015): A systematic literature review of the effect of carotid atherosclerosis on local vessel stiffness and elasticity. Atherosclerosis 243, 211-222

Bokaba RP, Anderson R, Theron AJ, Tintinger GR (2017): Cigarette smoke condensate attenuates phorbol ester-mediated neutrophil extracellular trap formation. Afr Health Sci 17, 896-904

Borregaard N (2010): Neutrophils, from marrow to microbes. Immunity 33, 657-670

Branzk N, Lubojemska A, Hardison SE, Wang Q, Gutierrez MG, Brown GD, Papayannopoulos V (2014): Neutrophils sense microbe size and selectively release neutrophil extracellular traps in response to large pathogens. Nat Immunol 15, 1017-1025

Brill A, Fuchs TA, Savchenko AS, Thomas GM, Martinod K, De Meyer SF, Bhandari AA, Wagner DD (2012): Neutrophil extracellular traps promote deep vein thrombosis in mice. J Thromb Haemost 10, 136-144

Brinkmann V, Goosmann C, Kuhn LI, Zychlinsky A (2012): Automatic quantification of in vitro NET formation. Front Immunol 3, 413

Brinkmann V, Reichard U, Goosmann C, Fauler B, Uhlemann Y, Weiss DS, Weinrauch Y, Zychlinsky A (2004): Neutrophil extracellular traps kill bacteria. Science 303, 1532-1535

Brullmann DD, Pabst A, Lehmann KM, Ziebart T, Klein MO, d'Hoedt B (2012): Counting touching cell nuclei using fast ellipse detection to assess in vitro cell characteristics: a feasibility study. Clin Oral Investig 16, 33-38

Bryk AH, Prior SM, Plens K, Konieczynska M, Hohendorff J, Malecki MT, Butenas S, Undas A (2019): Predictors of neutrophil extracellular traps markers in type 2 diabetes mellitus: associations with a prothrombotic state and hypofibrinolysis. Cardiovasc Diabetol 18, 49

Caillon A, Trimaille A, Favre J, Jesel L, Morel O, Kauffenstein G (2022): Role of neutrophils, platelets, and extracellular vesicles and their interactions in COVID-19-associated thrombopathy. J Thromb Haemost 20, 17-31

Caudrillier A, Kessenbrock K, Gilliss BM, Nguyen JX, Marques MB, Monestier M, Toy P, Werb Z, Looney MR (2012): Platelets induce neutrophil extracellular traps in transfusion-related acute lung injury. J Clin Invest 122, 2661-2671

Chen AY, DeLano FA, Valdez SR, Ha JN, Shin HY, Schmid-Schonbein GW (2010): Receptor cleavage reduces the fluid shear response in neutrophils of the spontaneously hypertensive rat. Am J Physiol Cell Physiol 299, C1441-1449

Cheng CP, Herfkens RJ, Taylor CA (2003): Comparison of abdominal aortic hemodynamics between men and women at rest and during lower limb exercise. J Vasc Surg 37, 118-123

Cheng CP, Parker D, Taylor CA (2002): Quantification of wall shear stress in large blood vessels using Lagrangian interpolation functions with cine phase-contrast magnetic resonance imaging. Ann Biomed Eng 30, 1020-1032

Chiang N, Sakuma M, Rodriguez AR, Spur BW, Irimia D, Serhan CN (2022): Resolvin T-series reduce neutrophil extracellular traps. Blood 139, 1222-1233

Corriden R, Moshensky A, Bojanowski CM, Meier A, Chien J, Nelson RK, Crotty Alexander LE (2020): E-cigarette use increases susceptibility to bacterial infection by impairment of human neutrophil chemotaxis, phagocytosis, and NET formation. Am J Physiol Cell Physiol 318, C205-C214

Cowland JB, Borregaard N (2016): Granulopoiesis and granules of human neutrophils. Immunol Rev 273, 11-28

Dang PM, Stensballe A, Boussetta T, Raad H, Dewas C, Kroviarski Y, Hayem G, Jensen ON, Gougerot-Pocidalo MA, El-Benna J (2006): A specific p47phox -serine phosphorylated by convergent MAPKs mediates neutrophil NADPH oxidase priming at inflammatory sites. J Clin Invest 116, 2033-2043

de Oliveira S, Rosowski EE, Huttenlocher A (2016): Neutrophil migration in infection and wound repair: going forward in reverse. Nat Rev Immunol 16, 378-391

Dewitz TS, Hung TC, Martin RR, McIntire LV (1977): Mechanical trauma in leukocytes. J Lab Clin Med 90, 728-736

Diaz JA, Fuchs TA, Jackson TO, Kremer Hovinga JA, Lämmle B, Henke PK, Myers DD, Jr., Wagner DD, Wakefield TW (2013): Plasma DNA is Elevated in Patients with Deep Vein Thrombosis. J Vasc Surg Venous Lymphat Disord 1, 341-348.e341

Douda DN, Khan MA, Grasemann H, Palaniyar N (2015): SK3 channel and mitochondrial ROS mediate NADPH oxidase-independent NETosis induced by calcium influx. Proc Natl Acad Sci U S A 112, 2817-2822

Egesten A, Breton-Gorius J, Guichard J, Gullberg U, Olsson I (1994): The heterogeneity of azurophil granules in neutrophil promyelocytes: immunogold localization of myeloperoxidase, cathepsin G, elastase, proteinase 3, and bactericidal/permeability increasing protein. Blood 83, 2985-2994

Ekpenyong AE, Toepfner N, Chilvers ER, Guck J (2015): Mechanotransduction in neutrophil activation and deactivation. Biochim Biophys Acta 1853, 3105-3116

Erpenbeck L, Schön MP (2017): Neutrophil extracellular traps: protagonists of cancer progression? Oncogene 36, 2483-2490

Fuchs TA, Abed U, Goosmann C, Hurwitz R, Schulze I, Wahn V, Weinrauch Y, Brinkmann V, Zychlinsky A (2007): Novel cell death program leads to neutrophil extracellular traps. J Cell Biol 176, 231-241

Garrido-Urbani S, Bradfield PF, Lee BP, Imhof BA (2008): Vascular and epithelial junctions: a barrier for leucocyte migration. Biochem Soc Trans 36, 203-211

Giegold O, Ludwig RJ, Hardt K, Will J, Schon MP, Oostingh GJ, Pfeilschifter JM, Boehncke WH, Radeke HH (2009): Computer-aided analysis of cell interactions under dynamic flow conditions. Exp Dermatol 18, 238-245

Hampton MB, Kettle AJ, Winterbourn CC (1998): Inside the neutrophil phagosome: oxidants, myeloperoxidase, and bacterial killing. Blood 92, 3007-3017

Hentzen E, McDonough D, McIntire L, Smith CW, Goldsmith HL, Simon SI (2002): Hydrodynamic shear and tethering through E-selectin signals phosphorylation of p38 MAP kinase and adhesion of human neutrophils. Ann Biomed Eng 30, 987-1001

Hirneiss C, Schumann RG, Gruterich M, Welge-Luessen UC, Kampik A, Neubauer AS (2007): Endothelial cell density in donor corneas: a comparison of automatic software programs with manual counting. Cornea 26, 80-83

Hohmann T, Dehghani F (2019): The Cytoskeleton-A Complex Interacting Meshwork. Cells 8

Hom G, Graham RR, Modrek B, Taylor KE, Ortmann W, Garnier S, Lee AT, Chung SA, Ferreira RC, Pant PV et al. (2008): Association of systemic lupus erythematosus with C8orf13-BLK and ITGAM-ITGAX. N Engl J Med 358, 900-909

Horobin JT, Watanabe N, Hakozaki M, Sabapathy S, Simmonds MJ (2019): Shear-stress mediated nitric oxide production within red blood cells: A dose-response. Clin Hemorheol Microcirc 71, 203-214

Hu SC, Yu HS, Yen FL, Lin CL, Chen GS, Lan CC (2016): Neutrophil extracellular trap formation is increased in psoriasis and induces human β-defensin-2 production in epidermal keratinocytes. Sci Rep 6, 31119

Huang D, Ding Q, Chen S, Lu S, Zhang Y, Long M (2021): E-selectin negatively regulates polymorphonuclear neutrophil transmigration through altered endothelial junction integrity. FASEB J 35, e21521

Hübner B, Lomiento M, Mammoli F, Illner D, Markaki Y, Ferrari S, Cremer M, Cremer T (2015): Remodeling of nuclear landscapes during human myelopoietic cell differentiation maintains co-aligned active and inactive nuclear compartments. Epigenetics Chromatin 8, 47

Immler R, Simon SI, Sperandio M (2018): Calcium signalling and related ion channels in neutrophil recruitment and function. Eur J Clin Invest 48 Suppl 2, e12964

Jackson MH, Millar AM, Dawes J, Bell D (1989): Neutrophil activation during cell separation procedures. Nucl Med Commun 10, 901-904

Jonuscheit S, Doughty MJ, Ramaesh K (2011): In vivo confocal microscopy of the corneal endothelium: comparison of three morphometry methods after corneal transplantation. Eye (Lond) 25, 1130-1137

Keitelman IA, Sabbione F, Shiromizu CM, Giai C, Fuentes F, Rosso D, Ledo C, Miglio Rodriguez M, Guzman M, Geffner JR et al. (2019): Short-Term Fever-Range Hyperthermia Accelerates NETosis and Reduces Pro-inflammatory Cytokine Secretion by Human Neutrophils. Front Immunol 10, 2374

Khan SQ, Khan I, Gupta V (2018): CD11b Activity Modulates Pathogenesis of Lupus Nephritis. Front Med (Lausanne) 5, 52

Kim TY, Gu JY, Jung HS, Koh Y, Kim I, Kim HK (2018): Elevated extracellular trap formation and contact system activation in acute leukemia. J Thromb Thrombolysis 46, 379-385

Kolaczkowska E, Kubes P (2013): Neutrophil recruitment and function in health and inflammation. Nat Rev Immunol 13, 159-175

Koutsiaris AG, Tachmitzi SV, Batis N, Kotoula MG, Karabatsas CH, Tsironi E, Chatzoulis DZ (2007): Volume flow and wall shear stress quantification in the human conjunctival capillaries and post-capillary venules in vivo. Biorheology 44, 375-386

Kouzarides T (2007): Chromatin modifications and their function. Cell 128, 693-705

Kuczia P, Zuk J, Iwaniec T, Soja J, Dropinski J, Malesa-Wlodzik M, Zareba L, Bazan JG, Undas A, Bazan-Socha S (2020): Citrullinated histone H3, a marker of extracellular trap formation, is increased in blood of stable asthma patients. Clin Transl Allergy 10, 31

Lawrence MB, Bainton DF, Springer TA (1994): Neutrophil tethering to and rolling on E-selectin are separable by requirement for L-selectin. Immunity 1, 137-145

Lee J, Luria A, Rhodes C, Raghu H, Lingampalli N, Sharpe O, Rada B, Sohn DH, Robinson WH, Sokolove J (2017): Nicotine drives neutrophil extracellular traps formation and accelerates collagen-induced arthritis. Rheumatology (Oxford) 56, 644-653

Leffler J, Gullstrand B, Jönsen A, Nilsson J, Martin M, Blom AM, Bengtsson AA (2013): Degradation of neutrophil extracellular traps co-varies with disease activity in patients with systemic lupus erythematosus. Arthritis Res Ther 15, R84

Liu H, Lan L, Abrigo J, Ip HL, Soo Y, Zheng D, Wong KS, Wang D, Shi L, Leung TW et al. (2021): Comparison of Newtonian and Non-newtonian Fluid Models in Blood Flow Simulation in Patients With Intracranial Arterial Stenosis. Front Physiol 12, 718540

Lyck R, Enzmann G (2015): The physiological roles of ICAM-1 and ICAM-2 in neutrophil migration into tissues. Curr Opin Hematol 22, 53-59

Makino A, Prossnitz ER, Bunemann M, Wang JM, Yao W, Schmid-Schonbein GW (2006): G protein-coupled receptors serve as mechanosensors for fluid shear stress in neutrophils. Am J Physiol Cell Physiol 290, C1633-1639

Malek AM, Alper SL, Izumo S (1999): Hemodynamic shear stress and its role in atherosclerosis. Jama 282, 2035-2042

Manley HR, Keightley MC, Lieschke GJ (2018): The Neutrophil Nucleus: An Important Influence on Neutrophil Migration and Function. Front Immunol 9, 2867

Metz RP, Patterson JL, Wilson E (2012): Vascular smooth muscle cells: isolation, culture, and characterization. Methods Mol Biol 843, 169-176

Metzler KD, Goosmann C, Lubojemska A, Zychlinsky A, Papayannopoulos V (2014): A myeloperoxidase-containing complex regulates neutrophil elastase release and actin dynamics during NETosis. Cell Rep 8, 883-896

Mitchell MJ, King MR (2012): Shear-induced resistance to neutrophil activation via the formyl peptide receptor. Biophys J 102, 1804-1814

Mitchell MJ, Lin KS, King MR (2014): Fluid shear stress increases neutrophil activation via platelet-activating factor. Biophys J 106, 2243-2253

Miyagi H, Stanley AA, Chokshi TJ, Pasqualino CY, Hoehn AL, Murphy CJ, Thomasy SM (2020): Comparison of automated vs manual analysis of corneal endothelial cell density and morphology in normal and corneal endothelial dystrophy-affected dogs. Vet Ophthalmol 23, 44-51

Murphy K, et al. (2012). Janeway's immunobiology. New York, Garland Science.

Neubert E, Bach KM, Busse J, Bogeski I, Schön MP, Kruss S, Erpenbeck L (2019): Blue and Long-Wave Ultraviolet Light Induce in vitro Neutrophil Extracellular Trap (NET) Formation. Front Immunol 10, 2428

Neubert E, Meyer D, Rocca F, Gunay G, Kwaczala-Tessmann A, Grandke J, Senger-Sander S, Geisler C, Egner A, Schon MP et al. (2018): Chromatin swelling drives neutrophil extracellular trap release. Nat Commun 9, 3767

Neubert E, Senger-Sander SN, Manzke VS, Busse J, Polo E, Scheidmann SEF, Schön MP, Kruss S, Erpenbeck L (2019): Serum and Serum Albumin Inhibit in vitro Formation of Neutrophil Extracellular Traps (NETs). Front Immunol 10, 12

Okuyama M, Ohta Y, Kambayashi J, Monden M (1996): Fluid shear stress induces actin polymerization in human neutrophils. J Cell Biochem 63, 432-441

Olins AL, Zwerger M, Herrmann H, Zentgraf H, Simon AJ, Monestier M, Olins DE (2008): The human granulocyte nucleus: Unusual nuclear envelope and heterochromatin composition. Eur J Cell Biol 87, 279-290

Omer-Cihangir R, Baser U, Kucukgergin C, Aykol-Sahin G, Huck O, Yalcin F (2021): Impact of Smoking on Neutrophil Enzyme Levels in Gingivitis: A Case-Control Study. Int J Environ Res Public Health 18

Papayannopoulos V (2018): Neutrophil extracellular traps in immunity and disease. Nat Rev Immunol 18, 134-147

Papayannopoulos V, Staab D, Zychlinsky A (2011): Neutrophil elastase enhances sputum solubilization in cystic fibrosis patients receiving DNase therapy. PLoS One 6, e28526

Pertiwi KR, de Boer OJ, Mackaaij C, Pabittei DR, de Winter RJ, Li X, van der Wal AC (2019): Extracellular traps derived from macrophages, mast cells, eosinophils and neutrophils are generated in a time-dependent manner during atherothrombosis. J Pathol 247, 505-512

Phillipson M, Heit B, Colarusso P, Liu L, Ballantyne CM, Kubes P (2006): Intraluminal crawling of neutrophils to emigration sites: a molecularly distinct process from adhesion in the recruitment cascade. J Exp Med 203, 2569-2575

Qiu SL, Zhang H, Tang QY, Bai J, He ZY, Zhang JQ, Li MH, Deng JM, Liu GN, Zhong XN (2017): Neutrophil extracellular traps induced by cigarette smoke activate plasmacytoid dendritic cells. Thorax 72, 1084-1093

Raup-Konsavage WM, Wang Y, Wang WW, Feliers D, Ruan H, Reeves WB (2018): Neutrophil peptidyl arginine deiminase-4 has a pivotal role in ischemia/reperfusion-induced acute kidney injury. Kidney Int 93, 365-374

Reidel B, Radicioni G, Clapp PW, Ford AA, Abdelwahab S, Rebuli ME, Haridass P, Alexis NE, Jaspers I, Kesimer M (2018): E-Cigarette Use Causes a Unique Innate Immune Response in the Lung, Involving Increased Neutrophilic Activation and Altered Mucin Secretion. Am J Respir Crit Care Med 197, 492-501

Rhodes B, Furnrohr BG, Roberts AL, Tzircotis G, Schett G, Spector TD, Vyse TJ (2012): The rs1143679 (R77H) lupus associated variant of ITGAM (CD11b) impairs complement receptor 3 mediated functions in human monocytes. Ann Rheum Dis 71, 2028-2034

Richmond TJ, Davey CA (2003): The structure of DNA in the nucleosome core. Nature 423, 145-150

Rochael NC, Guimarães-Costa AB, Nascimento MT, DeSouza-Vieira TS, Oliveira MP, Garcia e Souza LF, Oliveira MF, Saraiva EM (2015): Classical ROS-dependent and early/rapid ROS-independent release of Neutrophil Extracellular Traps triggered by Leishmania parasites. Sci Rep 5, 18302

Rossaint J, Herter JM, Van Aken H, Napirei M, Doring Y, Weber C, Soehnlein O, Zarbock A (2014): Synchronized integrin engagement and chemokine activation is crucial in neutrophil extracellular trap-mediated sterile inflammation. Blood 123, 2573-2584

Rouleau L, Rossi J, Leask RL (2010): Concentration and time effects of dextran exposure on endothelial cell viability, attachment, and inflammatory marker expression in vitro. Ann Biomed Eng 38, 1451-1462

Saito T, Takahashi H, Doken H, Koyama H, Aratani Y (2005): Phorbol myristate acetate induces neutrophil death through activation of p38 mitogen-activated protein kinase that requires endogenous reactive oxygen species other than HOCl. Biosci Biotechnol Biochem 69, 2207-2212

Schön MP, Erpenbeck L (2018): The Interleukin-23/Interleukin-17 Axis Links Adaptive and Innate Immunity in Psoriasis. Front Immunol 9, 1323

Serrano CV, Jr., Fraticelli A, Paniccia R, Teti A, Noble B, Corda S, Faraggiana T, Ziegelstein RC, Zweier JL, Capogrossi MC (1996): pH dependence of neutrophil-endothelial cell adhesion and adhesion molecule expression. Am J Physiol 271, C962-970

Simon DI, Chen Z, Xu H, Li CQ, Dong J, McIntire LV, Ballantyne CM, Zhang L, Furman MI, Berndt MC et al. (2000): Platelet glycoprotein ibalpha is a counterreceptor for the leukocyte integrin Mac-1 (CD11b/CD18). J Exp Med 192, 193-204

Skinner BM, Johnson EE (2017): Nuclear morphologies: their diversity and functional relevance. Chromosoma 126, 195-212

Son K, Small M, Sehmi R, Janssen L (2020): The eosinophil actin cytoskeleton undergoes rapid rearrangement in response to fluid shear stress. J Leukoc Biol 108, 129-137

Surolia R, Li FJ, Wang Z, Kashyap M, Srivastava RK, Traylor AM, Singh P, Dsouza KG, Kim H, Pittet JF et al. (2021): NETosis in the pathogenesis of acute lung injury following cutaneous chemical burns. JCI Insight 6

Takei H, Araki A, Watanabe H, Ichinose A, Sendo F (1996): Rapid killing of human neutrophils by the potent activator phorbol 12-myristate 13-acetate (PMA) accompanied by changes different from typical apoptosis or necrosis. J Leukoc Biol 59, 229-240

Tapper H (1996): The secretion of preformed granules by macrophages and neutrophils. J Leukoc Biol 59, 613-622

Thiam HR, Wong SL, Qiu R, Kittisopikul M, Vahabikashi A, Goldman AE, Goldman RD, Wagner DD, Waterman CM (2020): NETosis proceeds by cytoskeleton and endomembrane disassembly and PAD4-mediated chromatin decondensation and nuclear envelope rupture. Proc Natl Acad Sci U S A 117, 7326-7337

van Rees DJ, Szilagyi K, Kuijpers TW, Matlung HL, van den Berg TK (2016): Immunoreceptors on neutrophils. Semin Immunol 28, 94-108

Vorobjeva NV, Chernyak BV (2020): NETosis: Molecular Mechanisms, Role in Physiology and Pathology. Biochemistry (Mosc) 85, 1178-1190

Wang W, Peng W, Ning X (2018): Increased levels of neutrophil extracellular trap remnants in the serum of patients with rheumatoid arthritis. Int J Rheum Dis 21, 415-421

Warnatsch A, Ioannou M, Wang Q, Papayannopoulos V (2015): Inflammation. Neutrophil extracellular traps license macrophages for cytokine production in atherosclerosis. Science 349, 316-320

Yu X, Tan J, Diamond SL (2018): Hemodynamic force triggers rapid NETosis within sterile thrombotic occlusions. J Thromb Haemost 16, 316-329

Zarbock A, Ley K, McEver RP, Hidalgo A (2011): Leukocyte ligands for endothelial selectins: specialized glycoconjugates that mediate rolling and signaling under flow. Blood 118, 6743-6751

Zenaro E, Pietronigro E, Della Bianca V, Piacentino G, Marongiu L, Budui S, Turano E, Rossi B, Angiari S, Dusi S et al. (2015): Neutrophils promote Alzheimer's disease-like pathology and cognitive decline via LFA-1 integrin. Nat Med 21, 880-886

Acknowledgments

The work for this thesis would not have been possible without the support of a number of people.

I want to thank Prof. Dr. med. Michael P. Schön for the opportunity to work in his laboratory, for the constant support and inspiration during my work and the thorough review of my thesis. I also want to thank Prof. Dr. Sarah Köster for her commitment in supporting my project and her expertise on physical aspects of shear stress.

My special thanks go to Prof. Dr. med. Luise Erpenbeck for providing such an interesting topic for this experimental work, her great supervision throughout my work, her inspiring input and the support for presenting my project at the international convention "The neutrophil 2021" as well as for initiating the scholarship by the "Studienstiftung des deutschen Volkes".

To establish and adjust my experimental setup the help of Dr. Elsa Neubert is greatly appreciated. She introduced me to the field of neutrophil live cell experiments, was always keen to answer any questions and to discuss difficulties in the experimental setup and she inspired me in my approach to scientific projects.

For supporting my experiments, I want to thank all members of the AG Schön laboratory. Their constant help and goodwill strongly motivated me and the warm and humorous environment made every workday worthwhile. Special acknowledgments go to Meike Schraffinski for her technical support of my experiments.

Furthermore, I want to mention all members of the group of Prof. Dr. Sebastian Kruss, kindly supporting my project, offering very valuable advice on physical aspects, and providing access to their laboratory equipment.

For the opportunity to use their Ibidi circular pump system I am grateful to the group of Prof. Dr. Andreas Janshoff.

In addition, I want to thank my old friends Lasse Wulff for his great insight to understand fluid dynamics on a deeper level and Bennet Ströh for his excellent advice on statistical topics.

The always present support of my family and partner is greatly appreciated. I am thankful to my father, Ulrich Mrowietz, who constantly offered professional advice throughout my thesis in any aspect and for reviewing the first drafts of this work. I want to thank my mother, Sonja Mrowietz, and my brother Simon, who supported me by any means. And I am thankful to my partner, Julia Stölzner, who tirelessly encouraged me and with her steadfast loving support kept my spirits high even through the phase of isolation during challenging pandemic times.